

LITHIUM FLUORIDE ETCH MORPHOLOGIES
USING SILICA GEL

A STUDY OF LITHIUM FLUORIDE ETCH MORPHOLOGIES
USING SILICA GEL

BY

R. O. McELROY, B.Sc. (HONS.)

A Thesis

Submitted to the Faculty of Graduate Studies
in Partial Fulfilment of the Requirements
for the Degree
Master of Science

McMaster University

July 1967

MASTER OF SCIENCE (1967)
(Chemistry)

McMASTER UNIVERSITY
Hamilton, Ontario

TITLE: A Study of Lithium Fluoride Etch
Morphologies Using Silica Gel

AUTHOR: R. O. McElroy, B.Sc. (Hons.)
(University of Alberta)

SUPERVISOR: Dr. M. B. Ives

NUMBER OF PAGES: ix, 93

SCOPE AND CONTENTS: :

Cleavage surfaces of lithium fluoride are etched on a silica hydrogel containing ferric ions as inhibitor. The gel eliminates turbulence in the system and retards the diffusion of ferric ions towards the dissolving interface. The dissolution etch pits and features are examined by interference and electron microscopy. The ledge structure of pits thus formed is very regular. An explanation for the observed rounding of pits at high inhibitor concentration is proposed.

Acknowledgements

The author wishes to thank Dr. M. B. Ives for his aid and advice throughout the course of this project.

Thanks are extended to Mr. H. Walker and Mr. R. Jaracowitz for help with the replication technique and electron microscopy, and to Mrs. M. S. Baskin for assistance in the experimental work.

The author wishes to acknowledge the receipt of an Ontario Graduate Fellowship, and the support of a research grant from the United States Office of Naval Research.

TABLE OF CONTENTS

	Page
CHAPTER I.....	1
Introduction.....	1
Origins and Uses of Etch Pitting Studies.....	1
CHAPTER II.....	4
Surface Structure and Dissolution.....	4
Theory of Crystal Dissolution.....	4
Two Dimensional Nucleation.....	5
Dislocation Etch Pits.....	7
CHAPTER III.....	10
Dislocation Etch Pits on Lithium Fluoride.....	10
Introduction.....	10
Cation Inhibited Etching of Lithium Fluoride.....	11
Anion Inhibited Etching of Lithium Fluoride.....	13
CHAPTER IV.....	16
Factors Affecting Etch Pit Morphology.....	16
Kink Kinetics and Etch Morphologies.....	16
The Role of Diffusion in Etch Pit Rounding.....	19
Influence of Step Height on Dissolution Processes.....	21

	Page
CHAPTER V.....	24
Crystal Growth and Dissolution in Silica Gel...	24
Structure of Silica Gel.....	24
Crystal Growth in Gels.....	24
Etching of Crystals Using Silica Gel....	25
CHAPTER VI.....	28
Experimental Procedure.....	28
Materials and Techniques.....	28
Preparation and Treatment of Silica Gels.....	29
Etching on Silica Gels.....	30
Preparation of Replicas.....	30
CHAPTER VII.....	32
Results.....	32
Interference Microscope Study of Etched Surfaces.....	32
The Effect of pH on Etching.....	34
Electron Microscopy.....	34

	Page
CHAPTER VII.....	40
Discussion.....	40
Introduction.....	40
Effects of the Gel on Etching Behaviour.....	41
Stabilization of Rounded Ledges and Pits.....	44
Stabilization of Straight Ledges.....	48
Hydrochloric Acid Etching.....	49
Conclusions.....	50
Suggestions for Further Work.....	51
REFERENCES.....	52

LIST OF FIGURES

1. Features on a crystal surface.
2. Block model of (i) a ledge surface okl , and (ii) a kink surface hkl on an alkali halide crystal using Kossel's concept.
3. Dislocation etch pit structures on lithium fluoride with various etchants.
4. Typical adsorption isotherm for ferric ions adsorbed from saturated solutions on lithium fluoride surfaces.
5. Proposed structure for binuclear ferric ion species in aqueous solution.
6. Dissolution rate of the 100 surface of lithium fluoride as a function of ferric ion content (ppm) in the etchant.
7. Dependence on orientation of the free energy of a step at various temperatures.
8. A thermally etched sodium chloride surface, with monatomic and diatomic steps revealed by decoration with gold nuclei.
9. Kink kinetics
10. Crystal etching on a silica gel.

11. Interference micrographs of etch pits on lithium fluoride etched for 2 minutes at 10^4 ppm Fe^{+3} :
 - a. etched with stirring in silica free solution
 - b. etched without stirring in silica free solution
 - c. etched without stirring in equilibrated with silica gel
 - d. etched on silica gel equilibrated with etchant
12. Figure 11, with 10^3 ppm Fe^{+3} etchant.
13. Figure 11, with 10^2 ppm Fe^{+3} etchant.
14. Figure 11, with 10 ppm Fe^{+3} etchant.
15. Figure 11, with 5 ppm Fe^{+3} etchant.
16. Figure 11, with 0 ppm Fe^{+3} etchant.
17. Optical micrographs of lithium fluoride surfaces etched for 2 minutes with stirring in:
 - a. 1 N hydrochloric acid
 - b. 0.1 N hydrochloric acid
 - c. 0.01 N hydrochloric acid
 - d. 0.001 N hydrochloric acid
 - e. 0.0001
18. Interference micrograph of a lithium fluoride surface etched 2 minutes on a silica gel equilibrated with 10^4 ppm Fe^{+3} etchant.
19. 0 ppm Fe^{+3} stirred etch, 2 minutes.
20. 2 ppm Fe^{+3} stirred etch, 2 minutes.
21. 2 ppm Fe^{+3} stirred etch, 2 minutes.

22. 5 ppm Fe^{+3} stirred etch, 2 minutes.
23. 150 ppm Fe^{+3} stirred etch, 30 seconds.
24. 0 ppm Fe^{+3} gel etch, 5 minutes.
25. 10 ppm Fe^{+3} gel etch, 2 minutes.
26. 10 ppm Fe^{+3} gel etch, 2 minutes.
27. 100 ppm Fe^{+3} gel etch, 2 minutes.
28. 100 ppm Fe^{+3} gel etch, 2 minutes.
29. 100 ppm Fe^{+3} gel etch, 2 minutes.
30. 1000 ppm Fe^{+3} gel etch, 5 minutes.
31. 1000 ppm Fe^{+3} gel etch, 5 minutes.
32. 10,000 ppm Fe^{+3} gel etch, 2 minutes.
33. 10,000 ppm Fe^{+3} gel etch, 2 minutes.

CHAPTER I

Introduction

Origins and Uses of Etch Pitting Studies

Etch pitting techniques have been used by many investigators to study properties of ionic crystals. Studies of dislocation densities (1), segregation of impurities at dislocations (2), and movement of dislocations under stress (2,3), have all involved etch pitting of cleavage surfaces of ionic crystals.

Etch pitting techniques are also useful in studies on the kinetics (4,5,6), mechanisms, and inhibition of dissolution processes (6,7). These studies have usually involved cleavage surfaces of alkali halides, and comparatively simple etchants, but Ives (8) has pointed out that basic information on dissolution processes (especially the role of inhibitors) gained in studies on these simple systems may be applicable to problems involving corrosion of metals and dissolution of metal oxides.

In dissolution studies, dislocations, because of their finite free energy, serve as sites for formation of "two dimensional nuclei" or closed steps on a close packed surface (9).

Efforts have been made to correlate the shapes and sizes of resultant surface features to the macroscopic and microscopic processes associated with dissolution. Historically, the orientation of etch pits was used as a guide to crystal symmetries, since pit edges are normally in low index directions. However, the etch pit habits of some crystals are complicated functions of inhibitor concentration and solvent composition. Etching of sodium chloride can produce square pits in two orientations, octagonal pits, or conical pits (10), depending on the inhibitor and solvent composition.

Lithium fluoride surfaces can be etched to produce square pits in two orientations (2,11) or conical etch pits (figure 3).

The simplest etchant for lithium fluoride cleavages is an aqueous solution of a few parts per million (ppm) of ferric ions (2) (as ferric fluoride or chloride). In the concentration range 0.1-5 ppm Fe^{+3} , this etchant forms square pyramidal pits with edges in $\langle 100 \rangle$ directions on

lithium fluoride, but if $[\text{Fe}^{+3}] > 10$ ppm, interference (7), and electron microscopy studies show that the etch pits become conical in form.

There is no significant change in the net dissolution rate (13) or rate of increase in pit size corresponding to this change in morphology. There is, however, a considerable increase in the amount of iron adsorbed on the surface (7) in the range of inhibitor concentration where the pit shape changes from square to round. There is also a continuous increase in the surface ledge density with increasing inhibitor content of the etchant.

The aim of this research has been to provide an explanation for the observed rounding of etch pits (specifically on lithium fluoride) at high inhibitor concentrations. The principal technique used (etching on silica gels impregnated with etchant) was designed to test a previous hypothesis concerning the mechanism of pit rounding. The etched surfaces were examined by interference and electron microscopy in attempting to gain an understanding of the processes involved.

CHAPTER II

Surface Structure and Dissolution

Theory of Crystal Dissolution

Dissolution or evaporation of ionic crystals proceeds by the removal of ions from surface steps (14). Kossel (15) introduced the concept of a kink (see figure 1) on a monomolecular step, and suggested that during dissolution or evaporation ions would be removed from these sites since these ions have fewer nearest neighbours and are less strongly bound than ions elsewhere on a step or on a perfect surface.

It has been shown by Frenkel (16) and Burton and Cabrera (17,18) that kinks will form by thermal fluctuations on existing steps, but according to Burton and Cabrera (17,18), surface steps are not so easily formed. In fact, a perfect (dislocation free) crystal will remain essentially flat at temperatures up to the melting point.

Crystal edges can serve as sources of ledges for dissolution (but not for growth), and their role as a source of steps is shown by the rounding off of corners during dissolution.

Two Dimensional Nucleation

On a region of a perfect surface far from edges or dislocations, new steps can only be formed by a process of "two dimensional nucleation" (figure 1). The expression for the free energy of formation of a two dimensional nucleus consists of volume and free energy terms

$$\Delta G = \frac{r^2 h}{\Omega} \Delta \mu_0 + 2\pi r h \gamma \quad (i)$$

where r is the radius of the nucleus, h is the depth, γ is the surface energy (an average value) Ω is the atomic volume, and $\Delta \mu_0$ is the change in chemical potential when a molecule of the crystal goes into solution.

The radius ρ_c of the critical nucleus is defined by the condition that $\frac{dG}{dr} = 0$. Nuclei smaller than ρ_c will shrink, while nuclei larger than ρ_c will grow. The condition required for formation of a critical nucleus is therefore

$$\frac{2\pi \rho_c h}{\Omega} \Delta \mu_0 + 2\pi h \gamma = 0 \quad (ii)$$

The change in chemical potential is related to the undersaturation: $\Delta\mu_0 = kT \ln \frac{c}{c_0}$ where k is Boltzmann's constant, T the absolute temperature, c_0 the equilibrium concentration of solute and c the actual concentration. Substituting in the above equations gives

$$\rho_c = - \frac{\Omega \gamma}{kT \ln c/c_0} \quad (\text{iii})$$

the activation energy for two dimensional nucleation on a perfect surface is

$$G = - \frac{\pi \Omega \gamma^2 h}{kT \ln c/c_0} \quad (\text{iv})$$

At an edge dislocation, the free energy requirement for formation of a critical nucleus is less than that for a perfect surface because of the strain energy, $E(r)$, associated with the dislocation. $E(r)$ is the strain energy per unit length of a cylinder of radius r around the dislocation line. Therefore, free energy change for two dimensional nucleation at an edge dislocation is

$$G = \frac{\pi r^2 h \Delta\mu_0}{\Omega} + 2\pi r h \gamma' - hE(r) \quad (\text{v})$$

Since $E(r) > 0$, the activation energy for two dimensional nucleation at an edge dislocation will be lower than that on a perfect surface, and may be reduced to zero.

At the point of emergence of a screw dislocation, a step exists which cannot be eliminated by dissolution along the step.

The mechanisms for formation of etch features involve removal of atoms from a step terminating at a screw dislocation, or rapid two dimensional nucleation at an edge dislocation.

Dislocation Etch Pits

The profile of an etch feature depends on the relation between the rate of nucleation (v_n) of steps at a dislocation (or other imperfection) and the velocity of steps across the surface (v_s). If $v_s/v_n < 10$ the sides of the feature (or "pit") will have a slope of several degrees, and will be observable by optical or interferometric techniques. (19)

It has been suggested (20) that all etchants which produce observable etch pits contain, "by accident or design", an inhibitor which retards the step velocity. If the chemistry of the etchant is reasonably simple, the ratio v_s/v_n may be deliberately altered by changing the inhibitor concentration. Most etchants have been developed by trial and error methods, but Gilman et al. (2) and Moran (1) have attempted to deduce systematic criteria for deciding on inhibitors and solvents which will produce well

defined etch pits on ionic crystals. Inhibiting cations should be of nearly the same ionic radius as the cations of the substrate, and should form stable insoluble complexes with substrate anions (2). The solubility of the substrate in the solvent should be on the order of 0.05 - 0.2 g/100 ml (1).

The sides of etch pits do not normally correspond to crystallographic planes. The pit profiles of Ives and Hirth (4) show that the sides may be curved and the slope may be varied by changing the etchant composition. At low magnification, dislocation etch pits usually appear to be pyramidal with the apex of the pyramid on the dislocation line. Electron microscope studies (12) reveal that in some cases the interior surfaces of etch pits are composed of large low index planes separated by large steps of an irregular structure (figure 20).

The rate of dissolution at the tip of an etch pit will depend on the nature of the dislocation (Burger's vector and impurity content) and the etchant. On lithium fluoride, edge dislocations form deeper pits than screw dislocations, and dislocations containing segregated impurities etch more slowly than fresh dislocations (2).

If the nature of the etchant is such that rapid two dimensional nucleation occurs on the general surface, or the ledge velocity is much greater than the nucleation rate (i.e., $v_s \gg v_n$), then the width and depth of pits may be considerably altered. If surface dissolution is negligible, all pits should have the same diameter, but if surface dissolution is appreciable, then pit width will depend on v_n .

CHAPTER III

Dislocation Etch Pits on Lithium Fluoride

Introduction

As previously discussed, when a crystal dissolves in a solvent, two dimensional nuclei are formed preferentially at dislocations. The rate of movement of the steps formed is controlled by temperature, under-saturation of the solvent, and inhibition of the steps or kinks. In the absence of constraints such as inhibition or surface irregularities, steps and kinks travel rapidly until they are annihilated by meeting a kink or step moving in the opposite direction, or until they reach the edge of the surface. Such dissolution normally results in smooth surface features. In order to produce observable etch pits on a dissolving surface, it is necessary to slow down the step motion. This can be accomplished by adding to the solvent an inhibitor which will be preferentially adsorbed at kink sites, thus slowing the dissolution of ledges. A dislocation will provide a continuous source of surface steps, so under inhibited

conditions steps will pile up around the emergence point of the dislocation to form an etch pit.

There are three principal etchants for lithium fluoride cleavages: two of these involve cationic inhibitors (ferric ions) and one uses anionic inhibitors (fatty acids).

Cation Inhibited Etching of Lithium Fluoride

Gilman, Johnston and Sears (2) have exhaustively studied the formation of etch pits on lithium fluoride using cationic inhibitors. Of some thirty cations investigated, only Al^{+3} and Fe^{+3} were found to be effective. From this series of experiments, they concluded that to be a good inhibitor in this system, a cation must fulfil three conditions: it must have an ionic radius similar to that of the lithium ion, it must form a stable fluoride complex, and it should form a comparatively insoluble fluoride. These workers also showed that anions forming ferric or aluminium complexes more stable than the fluoride complex destroy the inhibiting action of the cation.

The normal etchant for lithium fluoride is an aqueous solution of 2-4 parts per million (ppm) of ferric ions (as ferric fluoride or chloride, although the anion is not important (2)), in distilled water acidified to

pH 2-3 to prevent precipitation of the ferric ions. This etchant has been referred to as the "W" etchant (5), and has been used to study mechanical properties of lithium fluoride by etching dislocations. The "W" etchant distinguishes between fresh and aged dislocations (deeper, more distinct pits are formed at the former (2)) and the shapes of the pits reveal the type of dislocation being etched. Edge dislocations form square pyramidal pits with edges parallel to $\langle 100 \rangle$ directions, while screw dislocations form slightly asymmetric pits. Figure 15a is an interference micrograph of a typical "W" etch.

Gilman and Johnston (11) first etched lithium fluoride with a modified CP-4 etchant consisting of equal volumes of concentrated hydrofluoric and glacial acetic acids saturated with ferric fluoride. This etchant (sometimes referred to as the "A" etchant (5)) forms square pyramidal pits with edges parallel to $\langle 110 \rangle$ directions, but does not distinguish between fresh and aged dislocations.

Ives (5) has investigated a simplified "A" type etchant consisting of a solution of ferric fluoride in concentrated hydrofluoric acid. The behaviour of this etchant parallels that of the "A" etchant.

Anion Inhibited Etching of Lithium Fluoride

Westwood and co-workers (21) have used aqueous solutions of C_7 , C_{13} and C_{17} fatty acids and fluorinated fatty acids to etch dislocations on lithium fluoride cleavages. The inhibiting action is presumably due to the interaction between the carboxyl anions and kinks or ledges on the crystal surface. The size of the inhibitor ions does not fit the criterion established by Gilman et al. (2) for inhibitor ions - it is much too large. However, lithium does form comparatively insoluble salts with fatty acids (22), a property similar to that of ferric and aluminium ions in forming stable sparingly soluble complexes with fluoride ions.

This technique produces square etch pits with edges in $\langle 100 \rangle$ directions. The pits formed are an order of magnitude smaller than those formed by etching for the same time in the "W" etchant. Westwood (21) suggests that since smaller pits are formed the fatty acids are the more effective inhibitors than ferric ions, but in the absence of evidence to the contrary, it seems possible that sufficient surface dissolution occurs to keep the pits small.

Initially, etch pits formed by the C_{13} and C_{17} (myristic and stearic) acids appear flat bottomed in optical micrographs, but they become pyramidal after a time. Westwood suggests that this effect is due to chemisorption of the inhibitor at the core of the dislocation. If chemisorption occurs near the core, it is likely to affect the ability of the core to function as a source of ledges. It seems possible that adsorption or chemisorption of a few long chain organic molecules near the area where critical nuclei are generated could effectively give the area a protective coating, since the long, hydrophobic carbon chains occupying the volume above the core could effectively limit access of solvent to the surface. As steps are slowly emitted, they will gradually pile up until finally the pit assumes a pyramidal form.

Electron Microscope Study of Lithium Fluoride Dissolution Morphology

Ramachandran and Ives (12) used high resolution electron microscopy to study lithium fluoride cleavages etched with stirring in the "W" etchant. Similar micrographs are shown in figures 20-23 . Their results showed that for etchant compositions in the range $Fe^{+3} = 1-5$ ppm the etch pit surfaces are not smooth

{ $0k\ell$ } planes (figure 2). The pit sides consist of comparatively high (0.01-0.05 μ) and regularly spaced steps. The areas between the steps were shown by shadowing measurements to be nearly {100} surfaces. The vertical portions of the steps, however, have a rough appearance (figure 21) with a considerable amount of substructure, indicating that travelling monatomic ledges have piled up or "bunched" behind an inhibited ledge.

Ramachandran and Ives (12) also observed that as the ferric ion concentration increases, the ledges become more closely spaced and less distinct. At concentrations greater than 10 ppm, the individual ledges can no longer be entirely resolved. This tendency to more closely spaced ledges corresponds to the transition in pit morphology from square pyramidal to conical. At ferric ion concentrations greater than 10 ppm the etch pits appear entirely conical in the interference microscope (figures 11-14 (a and b series)), and electron micrographs (figure 23) show a similar effect, although at the bottom of the pits there are, in some cases, remnants of a square pyramidal structure.

CHAPTER IV

Factors Affecting Etch Pit Morphology

Kink Kinetics and Etch Morphologies

The dissolution of ionic crystals can be thought of as proceeding by the solvation of ions at kink sites on the surface. The over-all morphology of etch features should, therefore, be determined by the rates of kink nucleation and travel on steps of various orientations. Ledges with orientations such that rates of kink nucleation and travel are rapid will dissolve rapidly and disappear, so the morphology of a closed step should be determined by the ledges which are most stable (i.e., have low rates of kink nucleation or travel, or are highly inhibited). In the critical nucleus which is assumed to be disc shaped, all ledge orientations should occur, but after a finite amount of dissolution, the step should assume the shape of the most stable ledges.

The rate of nucleation of kinks on a ledge is a function of temperature and the concentration of substrate in the solvent. Adsorption of an inhibitor ion at a kink site will hinder the dissolution of material from the kink. In fact, according to the electrostatic calculations of Gallily and Friedlander (23), the escape probability of an ion at an inhibited kink is lower than that of a ledge ion.

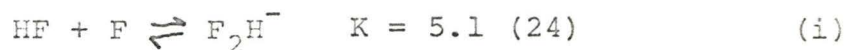
If we assume the rate of kink nucleation and mean lifetime (figure 9) to be variable parameters (5), then it should be possible to make some predictions about the equilibrium shape of a step.

Ives (5) has proposed two basic categories of kink kinetics which should give rise to different pit morphologies:

Type 1. "Little Inhibition" - If the mean time for kinks to sweep a ledge is less than the time between successive nucleation events in the ledge, then the unkinked ledge is stable and the rate of ledge motion will be determined by the kink nucleation rate.

Type 2. "Greater Inhibition" If the mean time for kink nucleation is less than the time required for a kink to sweep the ledge, then kinks should pile up to produce a "net kink ledge". In the limit of maximum kink density, an $\{hhl\}$ (figure 2) surface having ledges in $\langle 110 \rangle$ directions will be formed.

By studying the pits formed with "A" and "W" etchants separately and mixed in various proportions, Ives (5) proposed roles for each of the components of the etchants. Hydrofluoric acid increases the nucleation rate by increasing the effective undersaturation according to the reaction



Acetic acid reduced the solubility of the lithium fluoride, thus reversing the effect of the hydrofluoric acid, and the ferric ions acted as inhibitor. Ives (5) produced pits with morphologies corresponding to Type 1, and Type 2 kink kinetics. He also produced conical pits at high inhibitor levels (figure 3).

The Role of Diffusion in Etch Pit Rounding

Ives and Baskin (7) used a radio tracer technique to determine the adsorption isotherm for ferric ions on lithium fluoride cleavage surfaces. Their results (figure 4) showed that the transition from square to rounded pits at ferric ion concentrations above 5 ppm corresponds to a large increase in the amount of iron adsorbed on the surface. Since the development of conical pits suggests that crystallographic constraints on the shape of the pits are not the controlling factor, these workers proposed that diffusion rates of some species controlled the pit morphology. Kink nucleation and ledge motion are related to undersaturation (Appendix I) so a centrosymmetric diffusion field within the pit could lead to rounding of the ledges. The mechanism proposed was that the additional iron in solution formed complexes with fluoride ions at or near the surface. The presence of these large, sparingly soluble complexes hindered the diffusion of solvated ions away from the surface and/or the flux of solvent molecules approaching the surface. Once a diffusion barrier of some sort has been established it can be seen that kinks approaching a corner or another kink will be repelled (slowed down) by the diffusion fields of other

travelling kinks. This hypothesis is supported by the fact that the surface excess of iron increases continuously past the second inflection point on the isotherm (figure 4). At higher inhibitor concentrations, no deviation is observed at monolayer coverage ($\Gamma = 11$) (29). If the ferric ions were simply adsorbed at surface cation sites, some deviation in the isotherm would be expected at monolayer coverage. The absence of any inflection point at monolayer coverage indicates that the surface excess is in some other form - perhaps insoluble ferric fluoride complexes bounded to the surface through surface anions. Alternatively, the surface excess may consist of some hydrolysis product of the ferric ions. Even in the range of pH = 2-3 ferric ions tend to hydrolyze (25), and a dimeric structure (figure 5) has been suggested. Polymerization of this sort might account for the continuous increase in surface excess.

One experimental fact which is difficult to incorporate into a diffusion mechanism is the observation by Ives and Plewes (13) of the rate of dissolution of lithium fluoride as a function of ferric ion concentration in solution. As the ferric ion content of the solution increases the dissolution rate drops steeply until the "optimum" level (figure 6) is reached, and is fairly constant thereafter. If there is a growing diffusion barrier at the surface, the rate of dissolution would be

expected to decrease. It is possible, however, that kinetic measurements at high iron concentration do not adequately show any decrease in rate since dissolution under these conditions is so slow that very small quantities are being measured.

Influence of Step Height on Dissolution Processes

In a study of the molecular processes involved in crystal growth and evaporation using Kossel's (15) theory, Bethge (26) has used the technique of metal decoration to examine the behaviour of monatomic and diatomic steps on the surface of a sodium chloride cleavage after a small amount of evaporation. The monatomic steps are 2.81 \AA° high and are referred to as $a/2$ steps ("a" being the lattice constant). The diatomic (a) steps are 5.62 \AA° high. Evaporation spirals and patterns are formed around the emergence points in a manner analogous to formation of dissolution spirals (27) and etch pits on lithium fluoride, which has the same crystal structure.

Bethge (26) observed that all lamella systems (spirals and closed steps) having curved steps have a step height of $a/2$. The step heights of square lamellae are a (figure 8).

Keller (28) has given a theoretical explanation of the effect of the step height on step morphology. He observed that the step height influences the velocity of the ledge, as well as its shape. The $a/2$ (rounded) steps move approximately twice as fast as the steps of height a . Using the method of Lacmann (29), which involves determination of the energy required for removal of neutral groups from steps (quadrupoles from $a/2$ steps, octupoles from a steps), Keller (28) concluded that at a temperature of 0°K the equilibrium shape of closed steps on the NaCl type surface is a square independent of the step height. At higher temperatures, however, the free energy is increased for steps in all directions except $\langle 100 \rangle$. Again using the method of Lacmann (29) and considering configurational entropy, the increase in free energy for steps in the $\langle 110 \rangle$ direction was determined. The increase is small, but it is greater by a factor of ~ 2.5 for the $a/2$ steps than for the a steps. This result indicates that in the equilibrium shape of a closed $a/2$ step, the $\langle 110 \rangle$ ledges are more pronounced, so the corners should be more rounded than those of an a step. Keller (28) also implies that since all ledge orientations other than $\langle 100 \rangle$ are stabilized at higher temperatures, a blending

of many orientations should produce a round configuration. This prediction corresponds to the observations of Bethge (26) and Keller (28), that $a/2$ steps show considerable rounding, while a steps do not.

CHAPTER V

Crystal Growth and Dissolution in Silica Gel

Structure of Silica Gel

Silica gel is a three dimensional network of small crystals bonded by -Si-O-Si-O- chemical bonds (30) which in its as formed condition encloses the water present during gelation. A characteristic feature of gels is a network of pores. The diameter of these pores is a function of concentration and rate of gelation, but according to Planck (31), 1% silica gels have an average pore diameter of about 100 Å.

Crystal Growth in Gels

Recently Henisch and co-workers (32) have revived the technique of growing crystals in silica gels. This method makes possible the growth of large crystals for solid state experimentation and is used when the material to be crystallized has a low solubility in water and cannot be readily grown from

the melt or vapour. The principal purposes of the gel in crystal growth are: to prevent turbulence, to provide a volume where supersaturation can occur in the presence of a number of nucleation sites, and to permit reservoirs of the reagents to be separated so that steady state concentration gradients may be maintained.

Etching of Crystals Using Silica Gel

The ability of silica gel to eliminate turbulence in a system containing approximately 99% water, and the possibility of maintaining steady state diffusion gradients are of interest for dissolution studies. Turbulence due to stirring, convection or vibration near the surface of an etch pit will affect the degree of undersaturation and the availability of inhibitor near the surface, thus altering nucleation and growth rates of dissolution features.

If the surface of a crystal is in contact with a nonturbulent solvent medium, then after a time, a steady state situation will be reached in which there will be a diffusion gradient of substrate into the solution. If there is an inhibitor in the solvent which is strongly adsorbed on the crystal surface, there

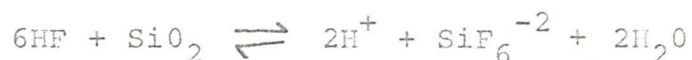
will be a diffusion of inhibitor particles towards the surface of the crystal since the inhibitor in the solvent volume near the surface will be depleted.

According to Henisch (33) the mobility of ions of low charge/radius ratio in silica gels is nearly the same as in water, but for highly charged ions, which are strongly hydrated, diffusivities will be appreciably lower because the large "hydrated radius" (34) of these ions limits movement of the ions through pores.

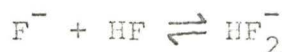
There is a possibility of highly charged cations being chemisorbed on silica gel at sites having replaceable hydrogen (Si-O-H) groups. However, Plank and Drake (35) have shown that Si-OH groups make up less than 1% of aged gels. Dalton and co-workers (40) have shown that when solutions of electrolytes such as ferric nitrate are exposed to dried silica gel and filtered, the resulting solution is enriched slightly in electrolyte. They interpret this result to mean that some small pores in gels are accessible to solvent molecules but not to the large hydrated ions. Plank (31) studied the adsorption of cations by silica gel and found that at pH = 3.0 silica gel showed zero

adsorption for ammonium ions, indicating that the gel functions as a very weak base.

Any acid solution containing fluoride ions may react with silica according to the equation



However, in very dilute aqueous solution, HF is a weak acid (36) and in dilute aqueous solution the reverse (hydrolysis) reaction is dominant. Also, fluoride ions decrease the acidity of HF by the reaction:



If, then, an as formed silica gel were impregnated with ferric ions, it should provide a medium free of turbulence. This medium should show what role diffusion processes play in the formation of dislocation etch pits on lithium fluoride.

CHAPTER VI

Experimental Procedure

Materials and Techniques

Crystals of lithium fluoride used in this work were supplied by the Harshaw Chemical Company, Cleveland, Ohio. The lithium fluoride was in a γ -irradiated condition for ease of cleaving. Experimental specimens were prepared by cleaving the bulk crystals along $\{100\}$ planes to produce platelets of approximately 5x5x1 mm. The $\{100\}$ surfaces were prepared by cleaving just prior to etching.

The method of Ives and Baskin (7) was used for samples etched under stirred conditions. All samples were etched at ambient temperature (70-75°F). Except for the series of etches in hydrochloric acid of pH = 0-4 (figure 17), all lithium fluoride samples were etched in a 0.1N hydrochloric acid (Mallinckrodt Reagent Grade) in distilled water, and containing various concentrations of ferric ions as ferric chloride (Fisher reagent grade).

Preparation and Treatment of the Silica Gels

The silica gels were made in 70x50 mm pyrex petri dishes by neutralizing 3 millilitres (ml) of a 10% by weight solution of sodium metasilicate (Fisher Reagent Grade $\text{Na}_2\text{SiO}_3 \cdot 9\text{H}_2\text{O}$) in distilled water with an equivalent volume of 1.0N hydrochloric acid. The gel composition was approximately 1% by weight of SiO_2 . The gels set within a few minutes, and were then rinsed free of sodium and chloride ions by allowing them to stand for several hours under each of three 50 ml portions of distilled water with occasional agitation.

The gels to be used for etching of lithium fluoride were then treated for several hours with three separate 25 ml portions of a solution containing 1% by weight (10^4 ppm) of iron as ferric chloride (Fisher Reagent Grade $\text{FeCl}_3 \cdot 6\text{H}_2\text{O}$) in 0.1N hydrochloric acid. The purpose of this was to ensure that any sites in the gel where ferric ions could be permanently chemisorbed would be saturated.

Gels to be used for etching at concentrations of less than 10^4 ppm Fe^{+3} were then equilibrated consecutively with several 25 ml portions of etchant of the desired concentration, so that the solution in

the pores of the gel would have the same composition as the supernatant solution. Equilibration appeared to be quite rapid since the ferric ion colour spread uniformly through gel and solution after an hour. All gels were equilibrated with at least six 25 ml portions and allowed to stand two hours under each portion.

Etching on Silica Gels

Etching of samples on the gels was done by placing a freshly cleaved crystal specimen on the surface of the gel under a sufficient depth of supernatant solution so that one face of the crystal would be etched in unstirred solution (figure 10). Thus comparisons could be made between etch pits formed at the gel-crystal interface and those formed at the solution-crystal interface.

Samples were etched for periods of two or five minutes, removed with forceps, rinsed (with vigorous agitation to remove any adhering particles of the gel) in absolute ethanol and diethyl ether, then dried in an air blast.

Preparation of Replicas

Samples whose surfaces were to be replicated for electron microscope examination were then rinsed for 30 seconds with strong agitation in a dilute suspension

of latex spheres of known diameter ($0.263 \pm .066 \mu$), then dried in an air blast. The latex spheres on the surface were used for calibration and pit slope measurements in the electron microscope study of the surface replicas.

All etched specimens were examined by interference microscopy. Gold-palladium shadowed graphite surface replicas were made for representative samples using the technique of Ramachandran and Ives (27). These replicas were examined in a Siemens Elmiskop I electron microscope at an accelerating voltage of 80 KV.

CHAPTER VII

Results

Interference Microscope Study of Etched Surfaces

Figures 11 to 16 show interference micrographs of lithium fluoride surfaces etched with varying quantities of inhibitor. The "a" series shows specimens etched with stirring in silica-free solutions; the "b" series shows specimens etched without stirring in silica free solution. The "c" series shows specimens etched in "supernatant" solution (i.e., etchant equilibrated with the gel), and the "d" series shows specimens etched on the gel. In each figure, the "c" and "d" photographs show opposite sides of the same specimen - one side etched in supernatant solution, the other side in contact with the gel (figure 10). Each interference line within the pits represents a vertical displacement of 0.27 microns on the surface.

The surfaces etched on gels show "barrelled" (rounded) pits at an inhibitor concentration of 10^4 ppm, but square pits at all other concentrations, except at 0 ppm Fe^{+3} where the surface features become shallow and indistinct. The surfaces etched in the supernatant solution equilibrated with the gel show round pits at all inhibitor concentrations above 5 ppm. At 5 ppm Fe^{+3} the surface shows square pits; at 0 ppm, the surface features are again shallow and indistinct.

The main difference between the "a" and "b" series is the size of the pits - specimens etched with stirring show larger pits in all cases. There is no distinct difference in pit morphology between these two series. Even at 5 ppm Fe^{+3} , where Gilman, Johnston and Sears (2) claimed that etching without stirring produced rounded pits, there is no distinct difference in pit morphology between figures 15a and 15b. The conflict with the results of Gilman et al. may not be significant, since these workers etched at a higher pH.

The morphologies of the pits in the "c" series are in all cases similar to those obtained by etching, with or without stirring, in silica free solutions.

The Effect of pH on Etching

In order to keep high concentrations of ferric chloride from hydrolyzing in solution, it was found necessary to add hydrochloric acid to lower the pH. To investigate any effect that hydrochloric acid alone might have on etching behaviour, samples of lithium fluoride were etched in solutions 1.0, 0.1, 0.01, 0.001, and 0.0001 N HCl. Figure 17 a-e shows optical micrographs of lithium fluoride surfaces etched with stirring for two minutes in each of these solutions.

No pits are formed, but the surface ledge structure at pH = 0 (figure 17a) shows some rounding. In the range pH = 1-3, (figure 17b-d) a number of square surface features occur. At a pH \geq 4, a uniform surface attack occurs.

Electron Microscopy

A representative selection of electron micrographs of etched and replicated lithium fluoride specimens is shown in figures 19-33.

Figures 19-23 show surfaces etched for two minutes under stirred conditions, so that the features of this type of etching can be compared to the surface features obtained by etching on silica gels.

Figure 19 (0 ppm Fe^{+3}) shows etching which has occurred in the vicinity of a surface step resulting from cleavage. The step still shows crystallographic alignment (the shadowing direction was approximately $\langle 100 \rangle$), but the surface of the specimen shows roughness indicative of general dissolution.

Figures 20, 21 and 22 show distinct etch pits. Figure 20 shows dissolution spirals (12) on the surface and a pit with three distinct ledges, each of which contains a considerable amount of resolved but disorderly substructure. The over-all shape of the pit is square, but the large steps have a curved envelope. For the inner step, the radius of curvature (determined geometrically from measurements on the print) is 4.8μ . The length of the step sides is 1.8μ (measured corner to corner) and the step height is 0.06μ (calculated from the length of shadow cast by the step and a known shadowing angle of 74°). Similar measurements for the second step show: radius of curvature = 7.4μ , pit side = 4.2μ , step height = 0.13μ .

Measurement of the shadow of the latex sphere (diameter = 0.27μ) shows that its length corresponds to a shadowing angle of 74° , indicating that the surface is $\{100\}$ and free of any substantial net density of unresolved steps.

Figure 21 shows the pit of figure 20 at higher magnification. The substructure of the ledges is rough, but in the corners where the resolution is best, it appears that the rounding is due to a pile-up of macro-kinks in the smaller constituent ledges.

Figure 22 (5 ppm Fe^{+3}) shows etch pits consisting of roughly square steps containing partially resolved substructure. The shadowing indicates that the steps (other than those near the center of the pits) are of approximately equal heights, but since they are not concentric (indicating that the character of the dislocation being etched is not pure edge), the spacing of ledges differs on different sides of the pit.

Figure 23 (reproduced by permission of T. R. Ramachandran) shows the rounded pits produced by etching with stirring at 150 ppm Fe^{+3} . The bottoms of the pits retain a square pyramidal configuration, but no individual steps are resolvable and the overall structure of the pits (as shown by interference microscopy - see figures 11a - 14a) is conical. This picture shows the typical features of specimens etched with stirring at ferric ion concentrations above 10 ppm.

Etching on a gel containing no ferric ions (figure 24) produces small surface steps, but no pits or other major features. The small shadowed artifacts on the surface of this and some other replicas are probably small particles of the silica gel not removed during washing.

Figures 25 and 26 show samples etched on silica gel containing 10 ppm Fe^{+3} . The pits are remarkably square and the ledges are very straight; the curvature is too slight to be measured by the geometrical method used to estimate the curvature of ledges formed in stirred etching. The heights of the ledges in the pit (figure 25) containing latex spheres range from 0.04μ to 0.08μ . The ledge heights tend to increase as ledges move away from the center of the pit, but the two outermost ledges do not fit this trend. The surface structures shown in figure 25 show some rounding and substructure as do some individual ledges in the pits. Figure 26 shows that the ledge spacing within pits is not entirely regular, and shows some rounding of general surface features. Dissolution spirals (27) are also noticeable.

Gel etching at 100 ppm (figures 27, 28, and 29) shows similar features - straight ledges within square pits, but some rounded features on the general surface. The ledges are more closely spaced, but still fully resolved at this inhibitor concentration.

At 1000 ppm ferric ion concentration, gel etching still produces square pits (figures 30 and 31), but no considerable rounding of the pits has occurred. Figure 31 shows the result of a five minute 1000 ppm gel etch in the vicinity of a flat bottomed pit (indicating that the dislocation has moved or terminated). In this case the ledges are again distinguishable. Figure 30 shows a large area at low magnification. The pits still appear square, but again the general surface features show more rounding. Figure 31 shows ledges within two adjacent pits. Where the ledges from the two pits run together, rounding appears again.

Figures 32 and 33 show gel etches at 10^4 ppm Fe^{+3} . At this inhibitor level, individual ledges within square pits are no longer fully resolvable, and shallow round pits appear. The round pit in figure 32 has an irregular profile shown by its line of intersection with the neighbouring square pit. The round pit in figure 33 is also shallower than neighbouring square

pits since the flat bottom indicates termination of the dislocation.

The fact that round and square pits co-exist on specimens etched on gels at 10^4 ppm can also be seen from figure 18.

CHAPTER VIII

Discussion

Introduction

The experimental technique of etching crystals on gels was devised to test the hypothesis (7) that a diffusion mechanism of some sort is responsible for the rounding of dislocation etch pits on lithium fluoride at high inhibitor concentrations. Some questions to be asked about the method and results are:

Does the method actually provide effective diffusion control at the dissolving surface?

What, if any, chemical or physical effects does the gel have, other than eliminating turbulence?

If diffusion is the only mode of mass transport at the gel-crystal interface, does diffusion control have any effect on ledge or pit morphology?

If diffusion control is not the factor leading to pit rounding, what other factor (or combination of factors) could have this effect?

Why does the presence of a regular diffusion field and/or high inhibitor concentration not significantly affect the rate of pit growth?

It is not yet possible to give definitive answers to all of these questions, but the results of the present work support some hypotheses.

Effects of the Gel on Etching Behaviour

If the silica gel retards the diffusion of ionic species to and from the dissolving surface, the efficiency of the inhibitor (at any given concentration) will be decreased because the ferric ions (due to their high charge/radius ratio) are strongly hydrated and will diffuse more slowly in gels than in free solution (33). Lithium and fluoride ions are also solvated, so their diffusivities may be inhibited to a lesser extent.

The results indicate that the gel restricts the access of ferric ions to the dissolving surface. The ledge heights and spacings of pits formed by etching in free solution decrease in size with increasing ferric ion concentration until at $\text{Fe}^{+3} = 150$ ppm, no individual ledges are resolvable (figure 23) with this electron microscope technique.*

*The limit of resolution with this method is approximately 0.02μ (200 Å).

For samples etched on gels, the same transition in ledge structure occurs over the range $\text{Fe}^{+3} = 10\text{-}10^4$ ppm, and even at 10^4 ppm, some ledge structure is still resolved (figure 32), indicating that insufficient inhibitor is reaching the surface to stabilize the number of microledges required to form a smooth surface.

The interference micrographs (figures 11-16) show that the pits formed by etching on gels are at least as wide and deep as those formed by etching without stirring in free solution. This indicates that the rates of diffusion of lithium and fluoride ions are not substantially altered by the presence of the gel.

Measurements of the mobilities of ferric, lithium, and fluoride ions in silica gel, and determination of the net amount of surface dissolution would be necessary to provide verification for these conclusions.

It is possible that the silica may react with the fluoride ions present in acid solution, thus decreasing the fluoride ion concentration near the gel-crystal interface. However, in dilute aqueous solution, hydrofluoric acid is a weak acid (24) and the reaction:



is strongly reversed at high water concentrations (36). Also, no deterioration of the gels was observed, even after long etching times. It is unlikely, therefore, that the silica undergoes any significant chemical reaction.

Any chemisorption of ferric ions by the gels was compensated for by treating all gels with several portions of etchant containing 10^4 ppm Fe^{+3} (to saturate any sites where iron might be permanently chemisorbed) before equilibrating with etchant of the desired inhibitor concentration.

The presence of the gel does not appear to physically restrict the access of the solvent to the dissolving surface. The pits observed have a regular structure, indicating that the gel has not prevented the solvent from reaching all parts of the surface. Some samples show "artifacts" (shadowed material protruding from the crystal surface). There is no disruption of the ledge structure corresponding to these features, so they are presumably dehydrated particles of the gel or extraneous material picked up by the sample during interferometric examination or replication.

Stabilization of Rounded Ledges and Pits

The purpose of the silica gel in this work was to eliminate turbulence in the etchant system, thus setting up a steady state diffusion field to test the hypothesis (7) that a diffusion mechanism controls the observed rounding of dislocation etch pits at high inhibitor concentrations. The samples etched on gels show very square pits at ferric ion concentrations up to 1000 ppm in this medium, so apparently some mechanism other than diffusion is responsible for the rounding of the pits.

Burton and Cabrera (17), and Keller (28) have calculated equilibrium shapes for closed steps on crystal surfaces. The dependence on orientation of the free energy of a step (38) is shown in figure 7. From this it can be seen that ledge orientations in non close-packed directions are stabilized (relative to close packed ledges) at temperatures above 0°K due to the increase in configurational entropy of kinked steps. In other words, as ledges containing a number of kinks are stabilized, the equilibrium shape of a ledge becomes rounded.

The electrostatic calculations of Gallily and Friedlander (23) show that lattice ions at a kink site on a lithium fluoride surface become more stable than the ledge ions if a ferric ion is adsorbed at the kink. If kinked ledges are stabilized by inhibitor adsorption rather than by an increase in configurational entropy, then with increasing inhibitor coverage, ledges and pits should become increasingly rounded. This effect is observed in the present work and in other studies (12, 39), but the stability of straight ledges at low inhibitor coverages is still to be explained.

At low inhibitor levels (figures 20 to 22, and 25 to 29), only a limited number of macroledges (i.e., large enough to be resolved by electron microscopy), are stabilized within the pits observed. As the inhibitor concentration is increased, the number of individual ledges increases (and their size decreases) until they are no longer resolvable. Etching with stirring at 150 ppm Fe^{+3} produces pits whose surfaces appear quite smooth (figure 23). The increasing density of steps in the stirred etches corresponds to the increased rounding of the pits (figures 13 to 15).

Bethge (26) and Keller (28) have shown experimentally that on evaporated surfaces of sodium chloride, monatomic steps are rounded, while diatomic steps follow close packed directions to a much greater extent (figure 8). Using the method of Lacmann (29), Keller (28) showed that monatomic steps produced by evaporation could be expected to show rounding with less stabilization (i.e., at a lower temperature) than diatomic steps.

If stabilization of a ledge by inhibitor absorption is equivalent to stabilization due to increased entropy (ledge free energy is lowered in either case), then diatomic or larger steps should be less rounded than monatomic steps.

As the inhibitor coverage on lithium fluoride is increased, more ledges are stabilized (figures 25 to 33). Any significant density of monatomic steps will result in rounding of the pit. In the limit, as inhibitor coverage increases to the point where all (or nearly all) of the ledges are monatomic, the pit will be conical with smooth surfaces (except on the atomic scale).

A possible explanation for the nearly constant size of etch pits under varying inhibitor coverages is that as more ledges are stabilized, there are more ledge sites available for nucleation of kinks. When monatomic steps pile up into macroledges, the only effective site for kink nucleation is at the top of the ledge. Thus at high inhibitor coverage individual kinks and steps will move more slowly, but there will be more kinks and ledges undergoing dissolution at a given moment because of the increased probability of kink nucleation.

It is observed in figures 25, and 26, that the ledges on the surface of the specimen away from the pits show more rounding than ledges within the pits. In some cases (figures 28 and 31) individual ledges within pits also break away from the regular pattern and show curvature.

The rounding of surface ledges may be due to the greater availability of inhibitor for areas away from the pits (i.e., areas having a lower density of kinks to adsorb the available iron). There may also be local flaws in the gel due to mechanical shocks during handling. Any local flaw in the gel will give free solution access to the surface and lead to rounding.

In figure 31, two etch pits overlap, and the salient corner formed by this overlap is rounded. This is to be expected, since edges provide a source of kinks which can move in two directions. The effect is similar to the rounding of exterior edges in a dissolving crystal.

In the gel etches at 10^4 ppm Fe^{+3} , (figures 32 and 33) there are shallow round pits adjacent to deeper square pits. This may be explained by assuming that there is sufficient inhibitor present to stabilize round features if the dissolution rate is slow, (i.e., there will be fewer sites for the inhibitor to fill), but not enough inhibitor to cause rounding of deeper pits with this greater flux of ledges. This hypothesis is supported by the fact that in figure 32 the sides of the round pit appear smooth, but there are still resolvable ledges in the square pits. This indicates that the inhibitor has a lower effective concentration in the deeper pit, since the experiments show that decreasing ledge spacing corresponds to increasing inhibitor concentration.

Stabilization of Straight Ledges in Gel Etching

The most noticeable feature of the specimens etched on gels at $\text{Fe}^{+3} = 10 - 10^3$ ppm is the straightness and regularity of the ledges within the pits (figures 25-31).

This effect may be due to the complete lack of turbulence in the system. The stirred etches at low inhibitor concentration show somewhat rounded ledges which may be due to the flow of solvent across the surface (figures 20-22). There is less substructure in the ledges of gel etched samples than in ledges on samples etched with stirring (compare figures 22 and 25). According to Keller (28) the equilibrium shape of closed steps of height = a is square. This prediction agrees with the results of the present work, and since the difference between gel and stirred etching is the degree of turbulence, it seems probable that the curvature of ledges on samples etched with stirring (at low inhibitor concentrations (figures 20-22)) is due to the effect of solvent flowing over the surface.

Hydrochloric Acid Etching

The etching in hydrochloric acid (figure 17) was done as a preliminary experiment to determine the effect of hydronium ion concentration on surface features. Hydronium ion is a poor inhibitor for this system (2) - no pits are produced. However, the results are of interest since with increasing acidity the surface is first smooth (figure 17e), then shows some straight

ledge structures (figure 17 b,c,d), and at high acidity shows some rounded ledge structure (figure 17a). This indicates that even a poor inhibitor may, at high concentrations, affect the dissolution morphology.

Conclusions

- (1) Etching of lithium fluoride cleavages on silica gels containing "W" etchant produces square dislocation etch pits with edges in 100 directions at ferric ion (inhibitor) concentrations from 5 ppm to 10^4 ppm. The ledge structure in these pits is remarkably regular.
- (2) The presence of the gel has a two-fold effect on etching behaviour. The gel eliminates turbulence in the system, thus permitting a steady state concentration gradient to be established at the dissolving surface. The gel retards diffusion of ferric ions towards the surface, thus widening the range of inhibitor concentrations which produce square pits.
- (3) The rounding of dislocation etch pits on lithium fluoride at high inhibitor concentrations is due to the stabilization, by adsorbed inhibitor, of large numbers of monatomic steps whose equilibrium configuration is rounded.

Suggestions for Further Work

The method of etching crystals on gels produces very regular etch pits. This technique may be useful for etching and dissolution studies on other crystals such as sodium fluoride. Once the silica gel is formed, the water enclosed may be exchanged with water miscible solvents, so other alkali halides which are too soluble to be successfully etched in aqueous solutions may also be etched by this technique. It may also be possible to etch metallic crystals by this technique if no gas is evolved by the oxidizing agent in the etchant.

Electron microscope studies of other systems which show rounded etch pits may provide confirmation of the hypothesis that rounding of pits corresponds to stabilization of monatomic ledges.

Mossbauer spectroscopy using Fe^{57} adsorbed on lithium fluoride may give information on the chemical environment of adsorbed inhibitor ions.

REFERENCES

1. P. R. Moran, J. Appl. Phys., 29, 1768, (1958).
2. J. J. Gilman, W. G. Johnston and G. W. Sears, J. Appl. Phys. 29, 747, (1958).
3. V. B. Pariiskii, S. V. Lubenets and V. I. Startsev, Sov. Phys. Solid State, 8, 976, (1966).
4. M. B. Ives and J. P. Hirth, J. Chem. Phys. 33, 517, (1960).
5. M. B. Ives, J. Phys. Chem. Solids 24, 275, (1963).
6. N. A. Toropov and Yu. P. Udalov, Sov. Phys. Dok., 10, 259, (1965).
7. M. B. Ives and M. S. Baskin, J. Appl. Phys. 36, 2057, (1965).
8. M. B. Ives, I and E C, 57, 35, (1965).
9. W. G. Johnston, Prog. Ceram. Sci. 2, 1, (1961).
10. N. F. Kostin, S. V. Lubenets and K. S. Aleksandrov, Sov. Phys. Cryst. 6, 588, (1962).
11. J. J. Gilman and W. G. Johnston, "Dislocations and Mechanical Properties of Crystals" (John Wiley and Sons, New York, 1957), p. 119.
12. M. B. Ives and T. R. Ramachandran, Tech. Rept. No. 7, USONR Contract No. 3925(00), 1966.
13. M. B. Ives and J. T. Plewes, J. Chem. Phys. 42, 293, (1965).
14. W. G. Johnston, Reference (9), p. 31.

15. W. Kossel, Nach. Ges. Wiss. Gottingen, 137, (1927).
16. J. Frenkel, J. Phys. U.S.S.R. 9, 392, (1945).
17. W. K. Burton, N. Cabrera and F. C. Frank, Phil. Trans. Roy. Soc. London, A243, 299, (1951).
18. W. K. Burton and N. Cabrera, Disc. Farad. Soc. on Crystal Growth, 1, 30, (1949).
19. W. G. Johnston, Reference (9), p. 30.
20. F. C. Frank, "Growth and Perfection of Crystals" (John Wiley, New York, 1958), p. 411-18.
21. A. R. C. Westwood, H. Oppenhauser Jr., and D. J. Goldheim, Phil. Mag 6, 1475, (1961).
22. F. A. Cotton and G. Wilkinson, "Advanced Inorganic Chemistry", (John Wiley and Sons, New York, 1962), p. 165.
23. I. Gallily and S. K. Friedlander, J. Chem. Phys. 42, 1502.
24. F. A. Cotton and G. Wilkinson, Reference (22), p. 291.
25. F. A. Cotton and G. Wilkinson, Reference (22), p. 715.
26. H. Bethge, "Crystal Growth", ed. H. S. Peiser, Pergamon Press (1966), p. 623.
27. M. B. Ives and T. R. Ramachandran, J. Appl. Phys., 38, 2121, (1967).
28. K. W. Keller, Reference (26) p. 629.
29. R. Lacmann, "Adsorption et Croissance Cristalline", C.N.R.S., Paris, 1965, p. 195.
30. M. J. Vold and R. J. Vold, "Colloid Chemistry", Reinhold, New York, 1964, p. 108-109.
31. C. J. Plank, J. Coll. Sci., 2, 413, (1947).

32. H. K. Henisch, J. Dennis and J. I. Hanoka, J. Chem. Phys. Solids, 26, 493, (1965).
33. J. Dennis and H. K. Henisch, J. Elec. Chem. Soc., 114, 263, (1967).
34. C. J. Plank, J. Phys. Chem., 57, 284, (1953).
35. C. J. Plank and L. C. Drake, J. Coll. Sci., 2, 399, (1947).
36. F. A. Cotton and G. Wilkinson, Reference (22), p. 291.
37. F. A. Cotton and G. Wilkinson, Reference (22), p. 356.
38. F. C. Frank, "Metal Surfaces", A.S.M., Ohio, 1962, p. 10.
39. N. A. Toropov and Yu. P. Udalov, Sov. Phys. Dok. 10, 259, (1965).
40. R. W. Dalton, J. L. McClanahan, and R. W. Maatman, J. Coll. Sci., 17, 207, (1962).

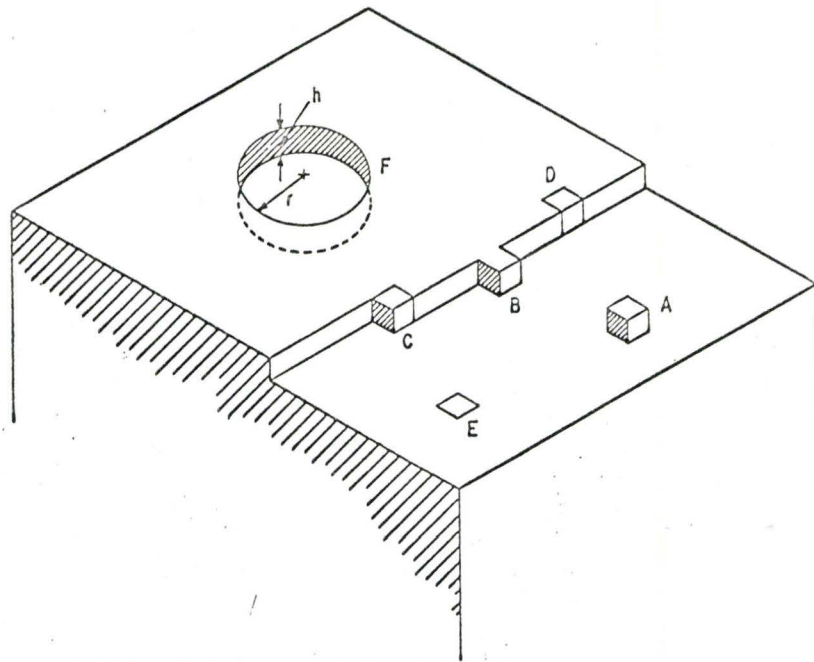
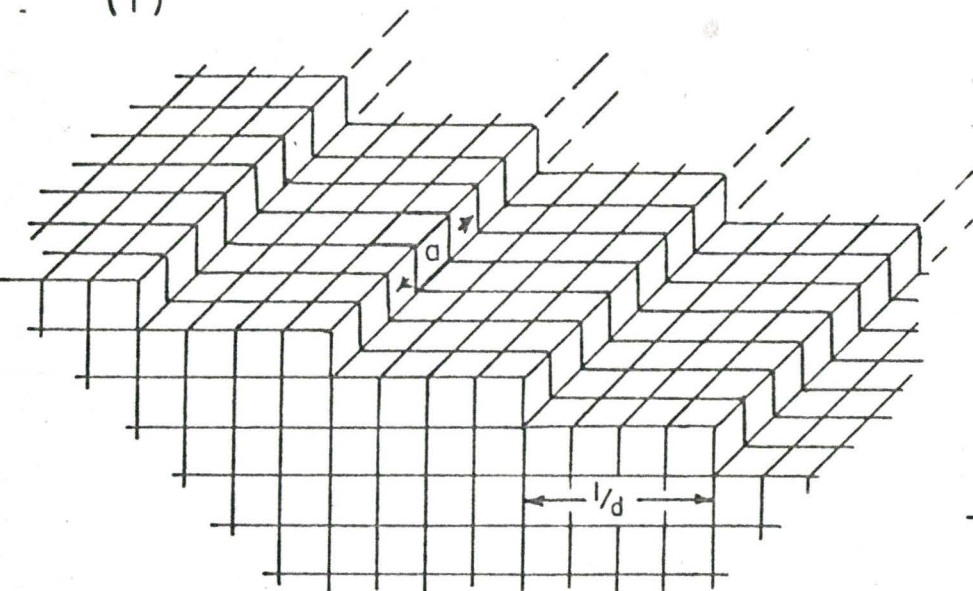


Figure 1

Sketch of features on a crystal surface. (A) Atom adsorbed on the surface. (B) Atom adsorbed at a monatomic step. (C) Atom at a kink in the monatomic step. (D) Atom in the step. (E) Atom in a perfect region of the surface. (F) Pit of radius, r , and monatomic depth, h .

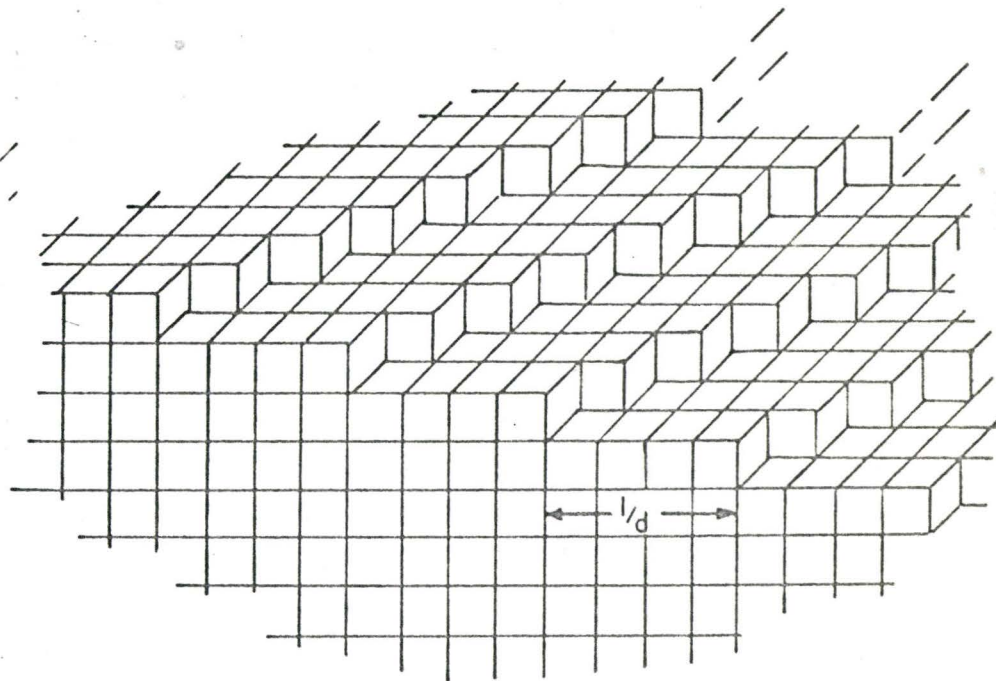
(Adapted from W. G. Johnston, *Prog. Ceram. Sci.*, 2, 1 (1962).)

(i)



$\{okl\}$

(ii)



$\{hhl\}$

Figure 2

Block model of: (i) a okl ledge surface, and (ii) a kink surface hhl on an alkali halide crystal using Kossel's concept.

(Adapted from M. B. Ives, J. Phys. Chem. Solids, 24, 275 (1963).)

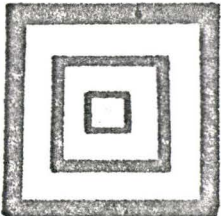
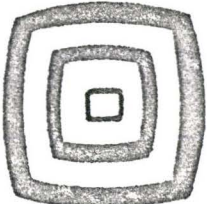
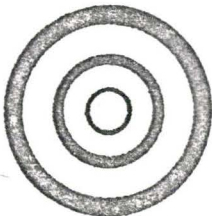
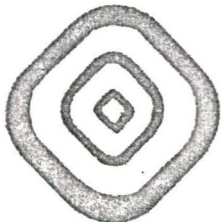
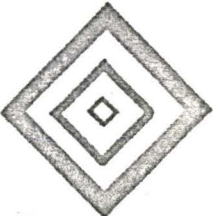
	(a)	(b)	(c)	(d)	(e)
INTERFERENCE PATTERN					
ETCHANT TYPE FOR LiF.	"W"	"W"(excess Fe ⁺⁺⁺)	"W" + HF	"W" + "F"	"F"

Figure 3

Dislocation etch pit structure on lithium fluoride with various etchants.

(Adapted from M. B. Ives, J. Phys. Chem. Solids, 24, 275, (1963).)

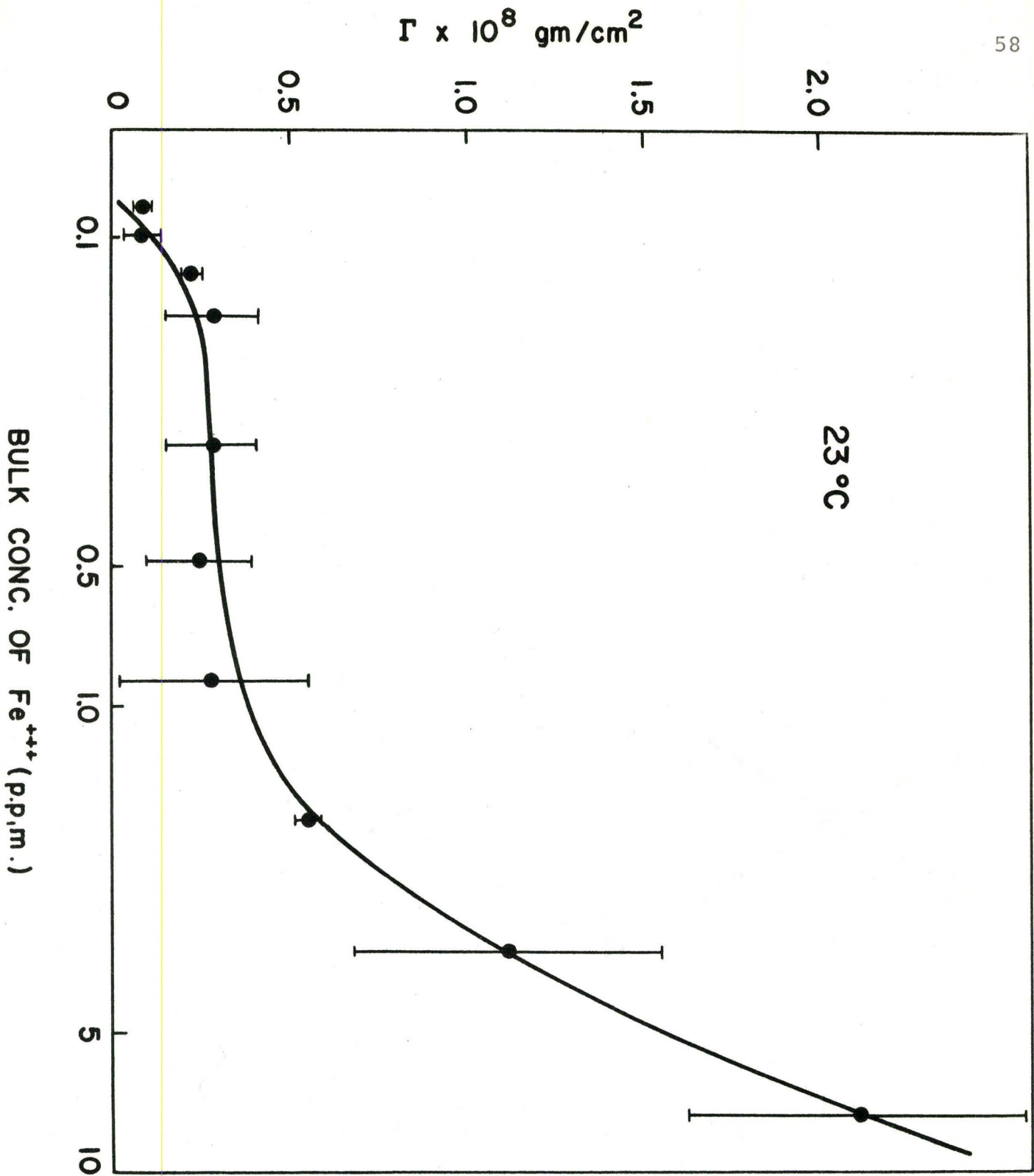


Figure 4

Typical adsorption isotherm for ferric ions adsorbed from saturated solutions on lithium fluoride surfaces.

(M. B. Ives and M. S. Baskin, *J. Appl. Phys.*, 36 2057, (1965).)

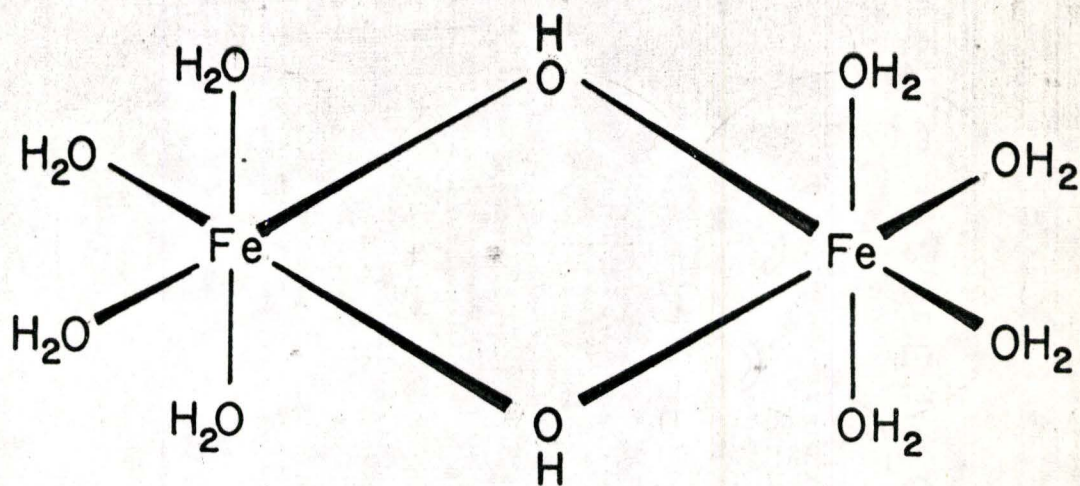


Figure 5: Proposed structure for a binuclear ferric ion species in aqueous solution (25).

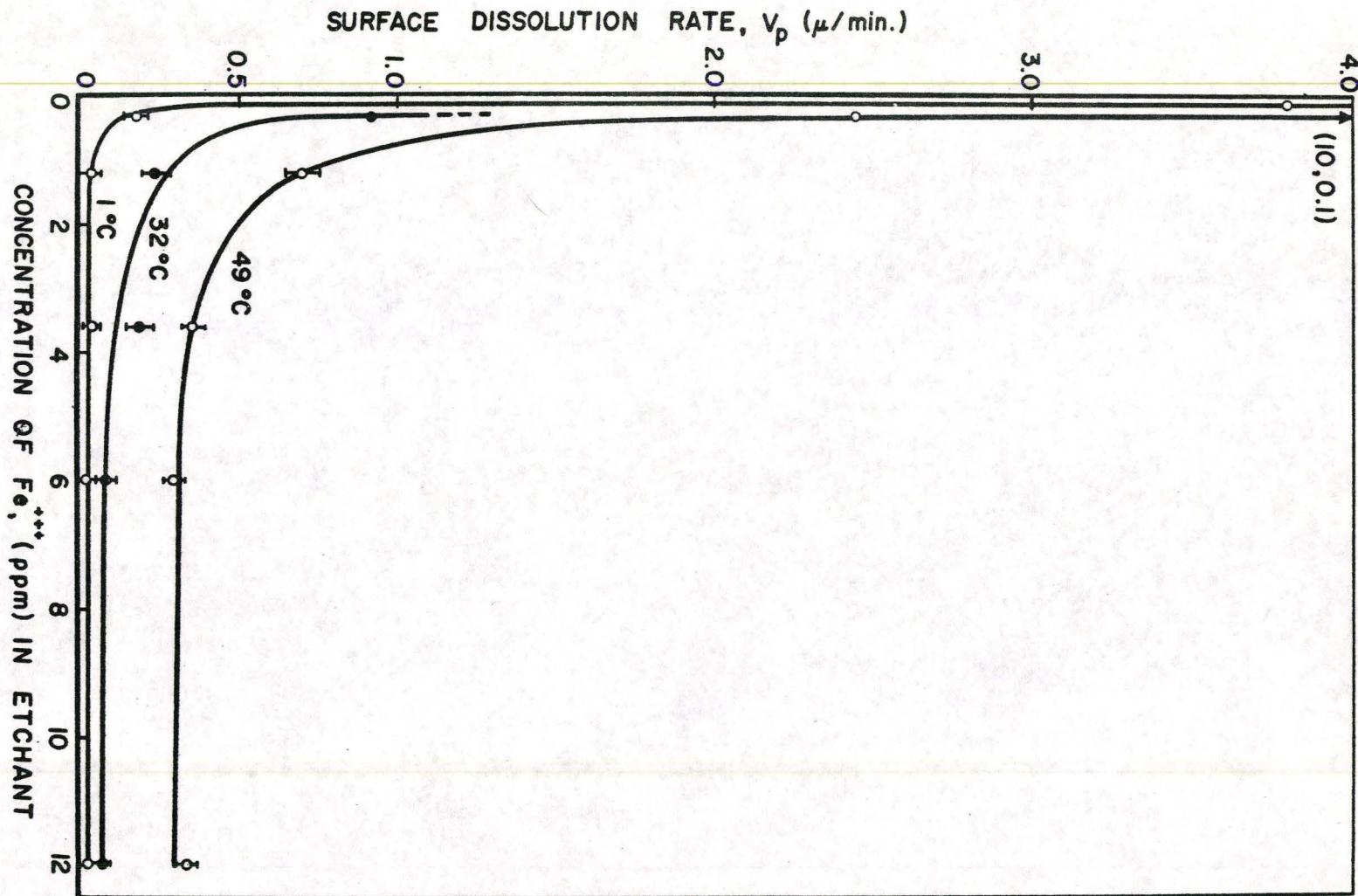


Figure 6

Dissolution rate of the {100} surface of lithium fluoride as a function of the ferric ion content of the etchant.

(M. B. Ives and J. T. Plewes, J. Chem. Phys., 42, 293 (1965).)

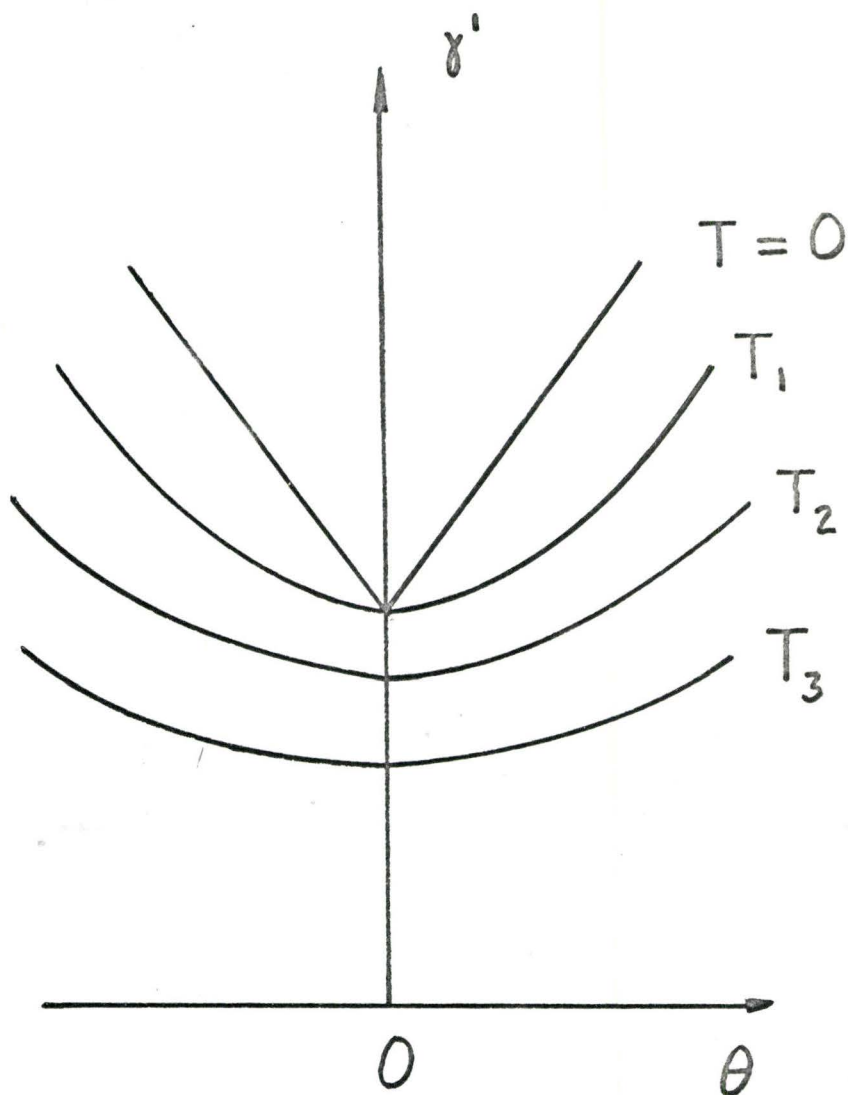


Figure 7

Dependence on orientation of the free energy of a step at $T = 0^\circ\text{K}$, and three successively higher temperatures (schematic). Theta equals zero is the kinkless direction for the step at $T = 0^\circ\text{K}$.

(F. C. Frank, "Metal Surfaces", A.S.M., 1963, p. 10.)

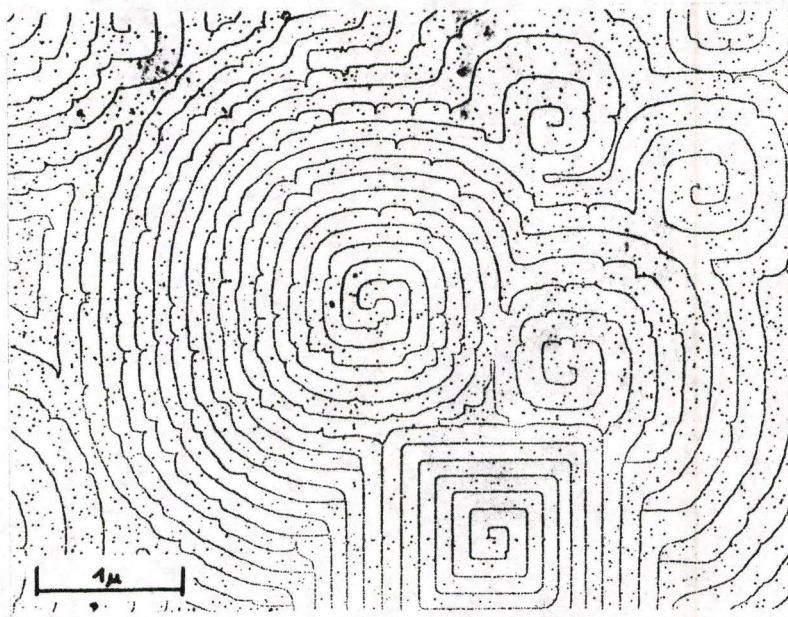


Figure 8

A thermally etched sodium chloride surface, with monatomic and diatomic steps decorated by gold nuclei (26).

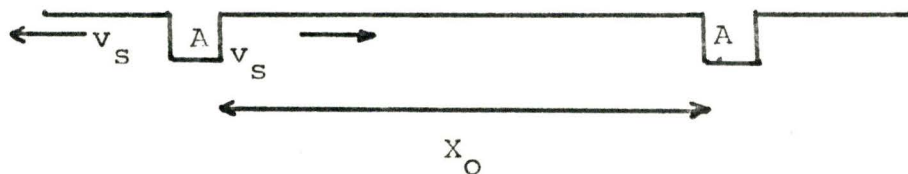


Figure 9

Kink Kinetics: Top view of a moving ledge.

(A) Double kink (kink pair).

(v_s) Mean velocity of a kink.

(X_0) Mean spacing of nucleation sites.

Definitions: Mean lifetime of a kink =

$$= X_0 / 2v_s$$

Nucleation^s frequency = $1/t$

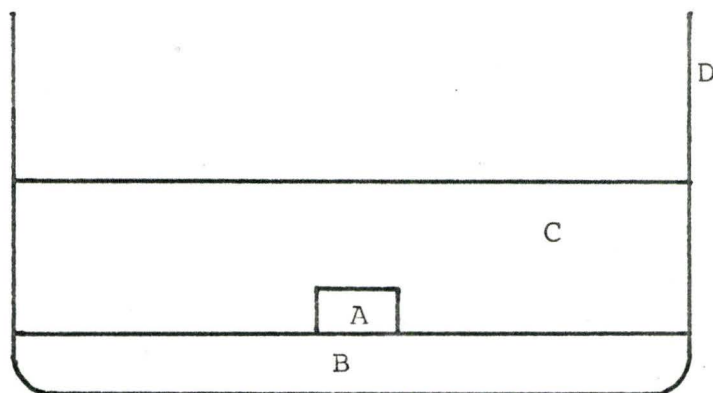


Figure 10

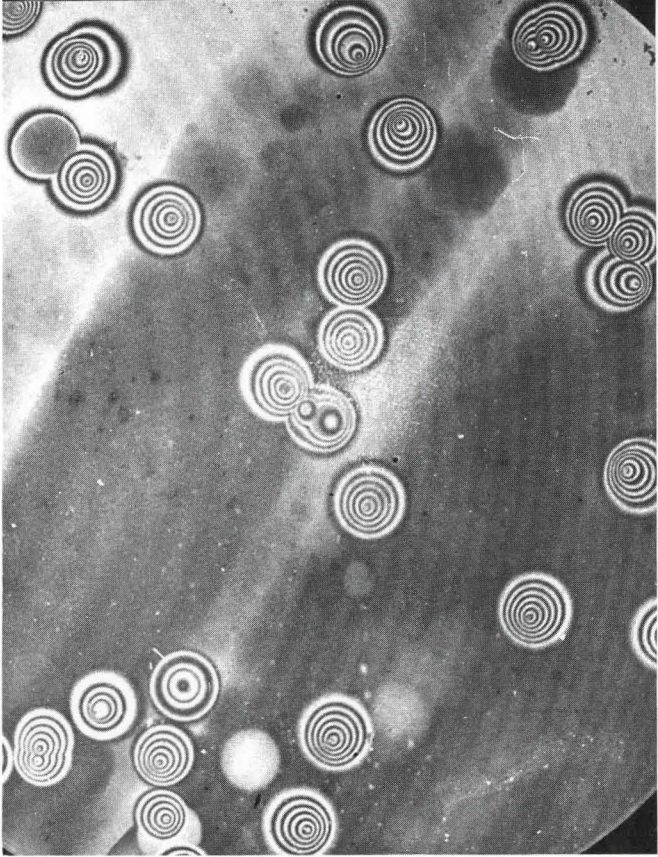
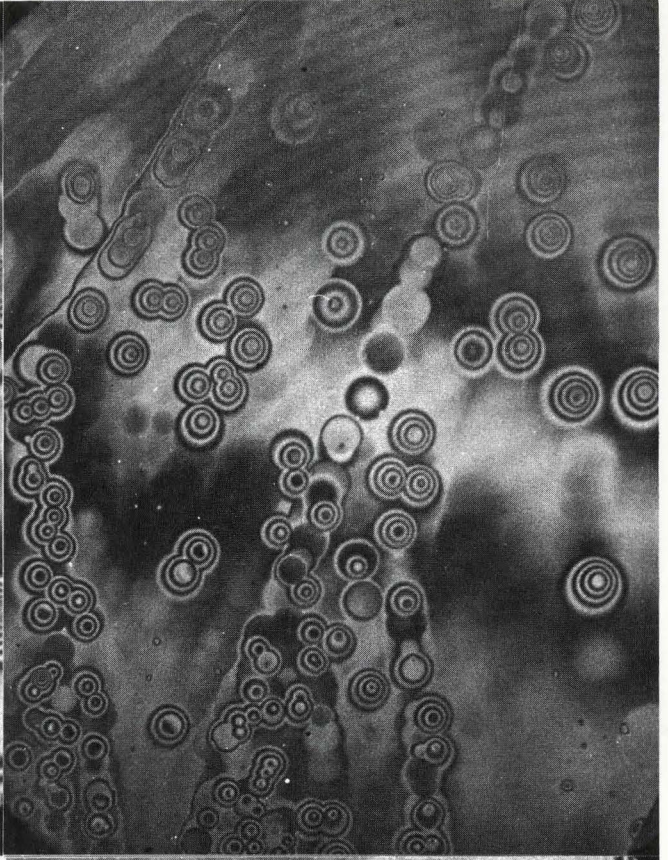
Crystal etching on a silica gel.
(A) Dissolving crystal. (B) Silica gel. (C) Supernatant etchant.
(D) Petri dish.

Figure 11: Interference micrographs of lithium fluoride surfaces etched 2 minutes at 10^4 ppm.

- Fe^{+3} :
- a. With stirring.
 - b. Without stirring.
 - c. In supernatant solution.
 - d. On silica gel. (500 X).

a

b



c

d

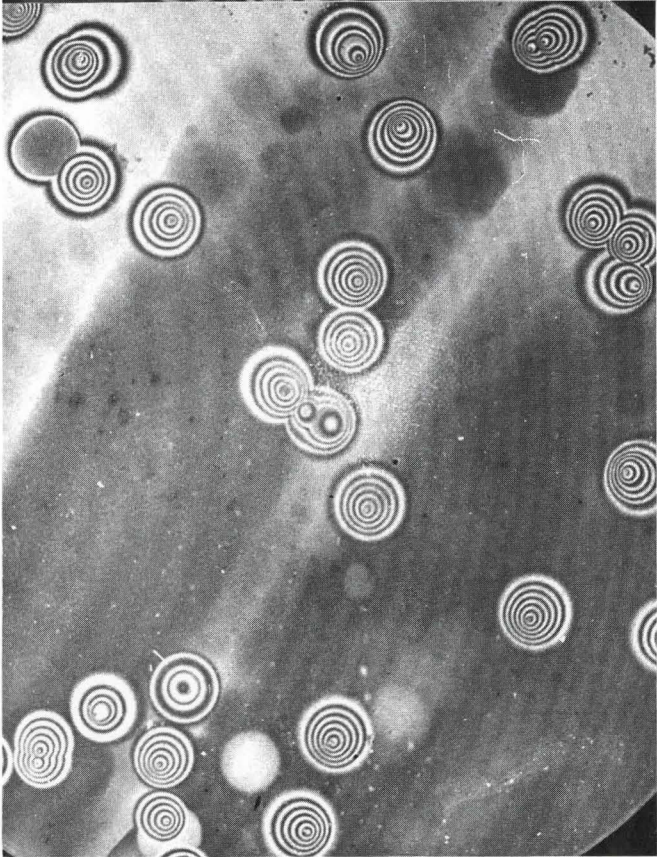
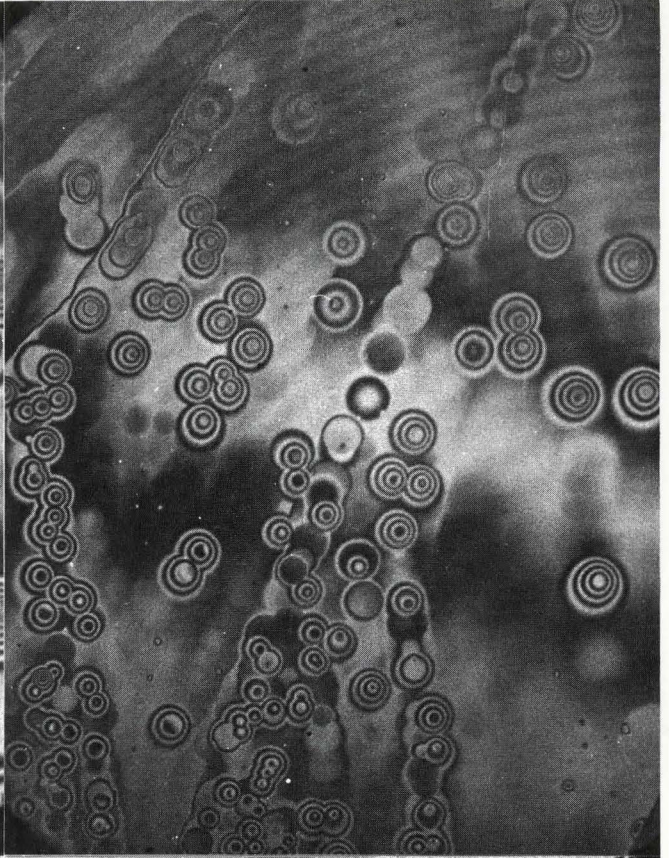
Figure 12

Figure 12: Interference micrographs of lithium fluoride surfaces etched 2 minutes at 10^3 ppm.

- Fe^{+3} :
- a. With stirring.
 - b. Without stirring.
 - c. In supernatant solution.
 - d. On silica gel. (500 X).

a

b



c

d

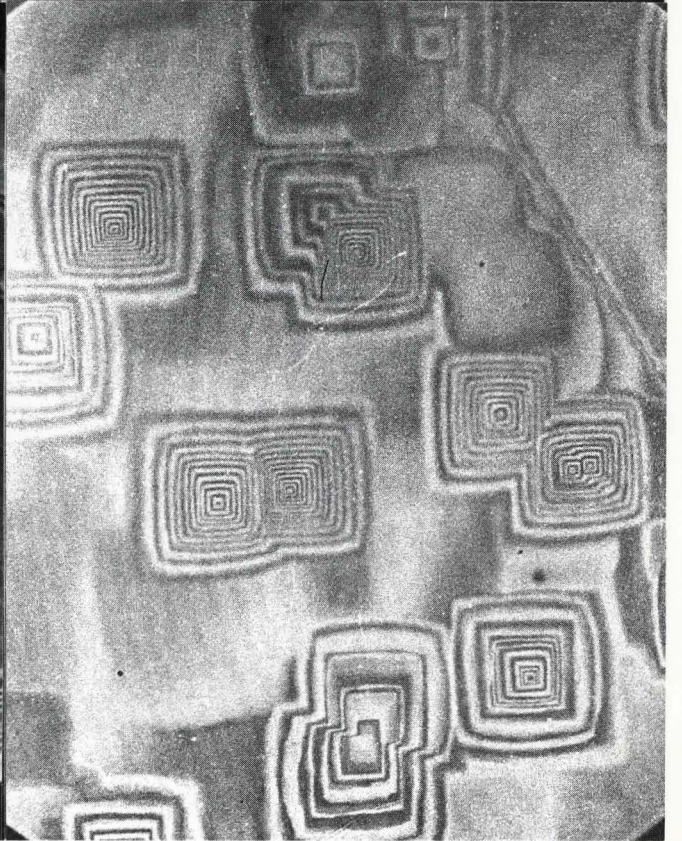
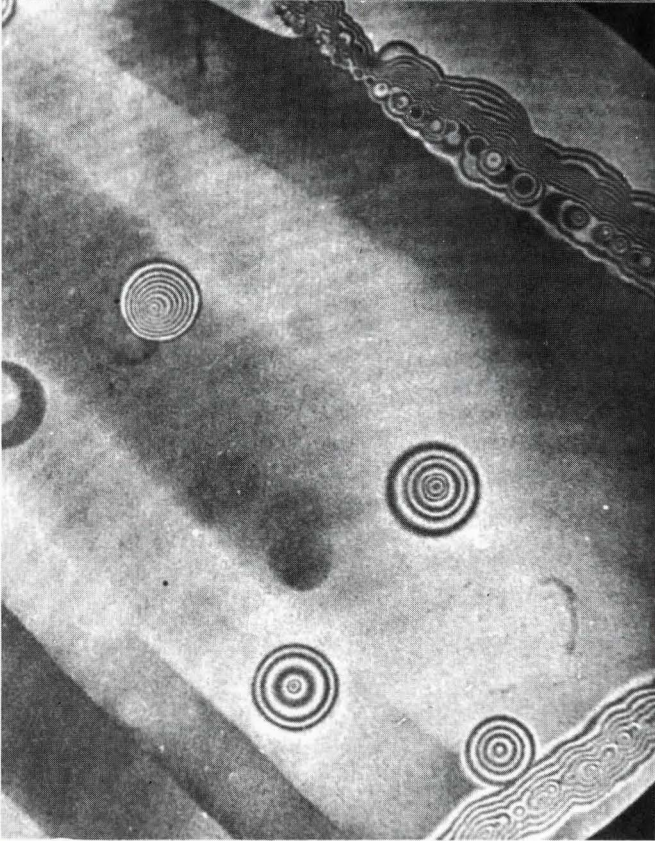
Figure 12

Figure 13: Interference micrographs of lithium fluoride surfaces etched 2 minutes at 10^2 ppm.

- Fe^{+3} :
- a. With stirring.
 - b. Without stirring.
 - c. In supernatant solution.
 - d. On silica gel. (500 X).

a

b



c

d

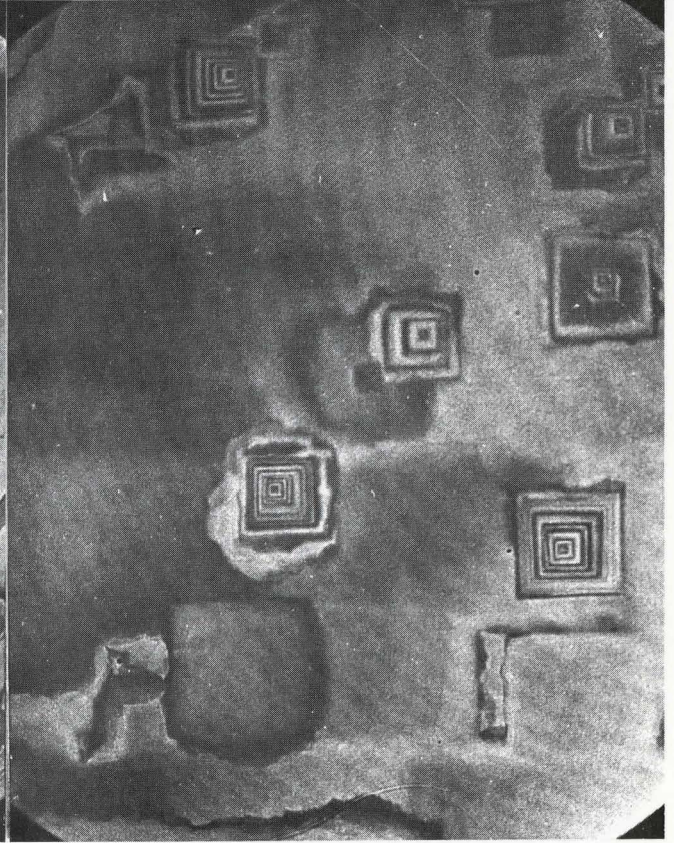
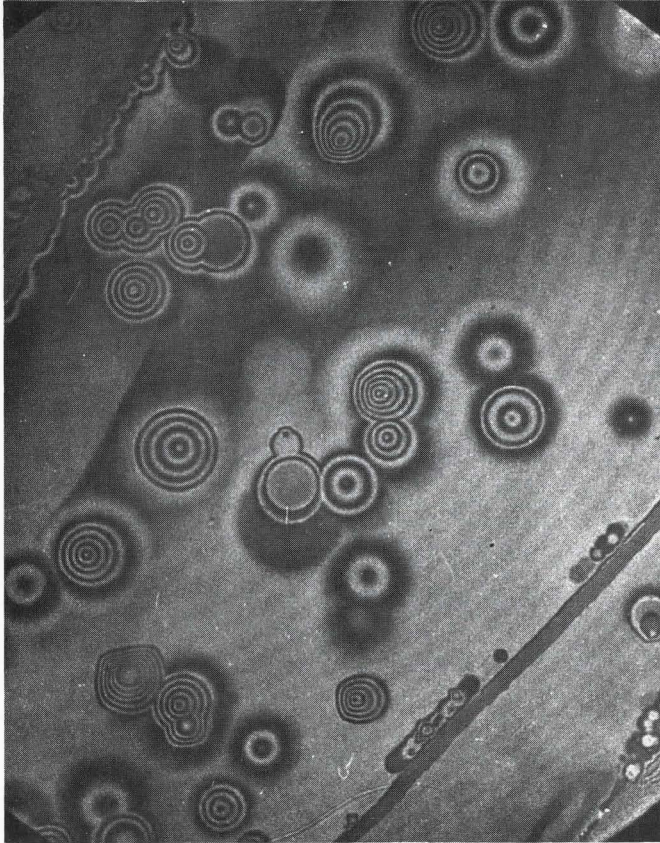
Figure 13

Figure 14: Interference micrographs of lithium fluoride surfaces etched 2 minutes at 10 ppm.

- Fe⁺³:
- a. With stirring.
 - b. Without stirring.
 - c. In supernatant solution.
 - d. On silica gel (500 X).

a

b



c

d

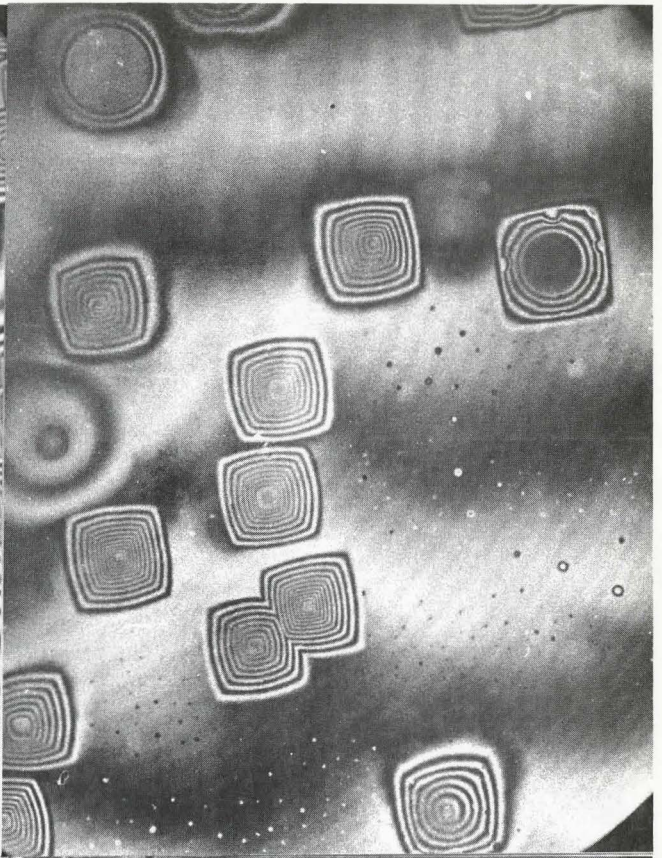
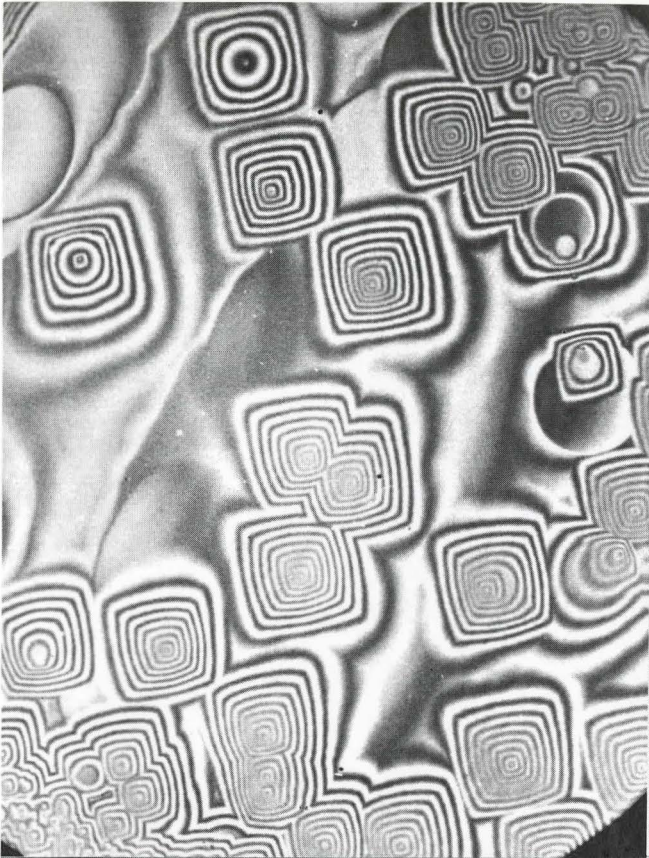
Figure 14

Figure 15: Interference micrographs of lithium fluoride surfaces etched 2 minutes at 5 ppm.

- Fe^{+3} :
- a. With stirring.
 - b. Without stirring.
 - c. In supernatant solution.
 - d. On silica gel (500 X).

a

b



c

d

Figure 15

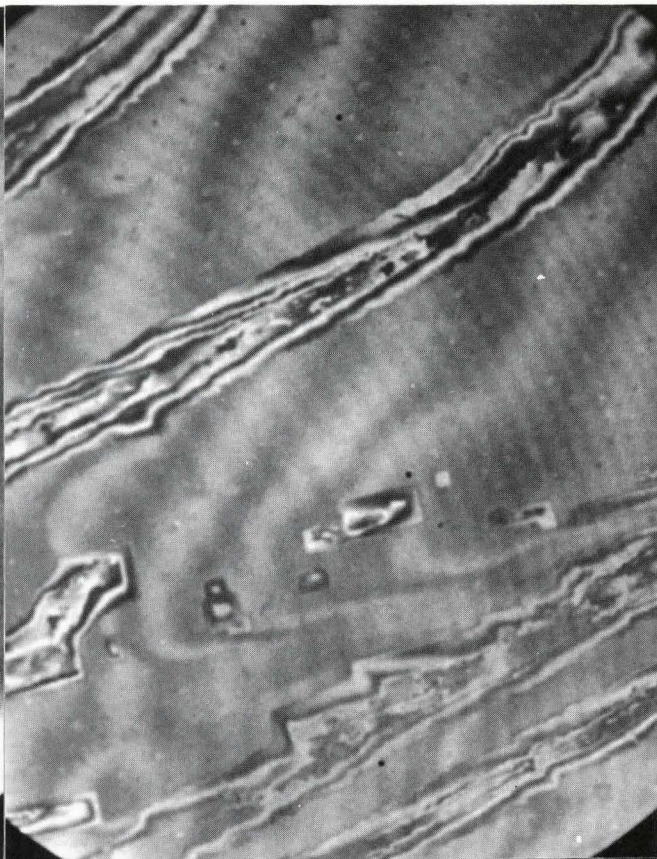
Figure 16: Interference micrographs of lithium fluoride surfaces etched 2 minutes at 0 ppm.

- Fe⁺³:
- a. With stirring
 - b. Without stirring.
 - c. In supernatant solution.
 - d. On silica gel (500 X).

a

b

76



c

d

Figure 16

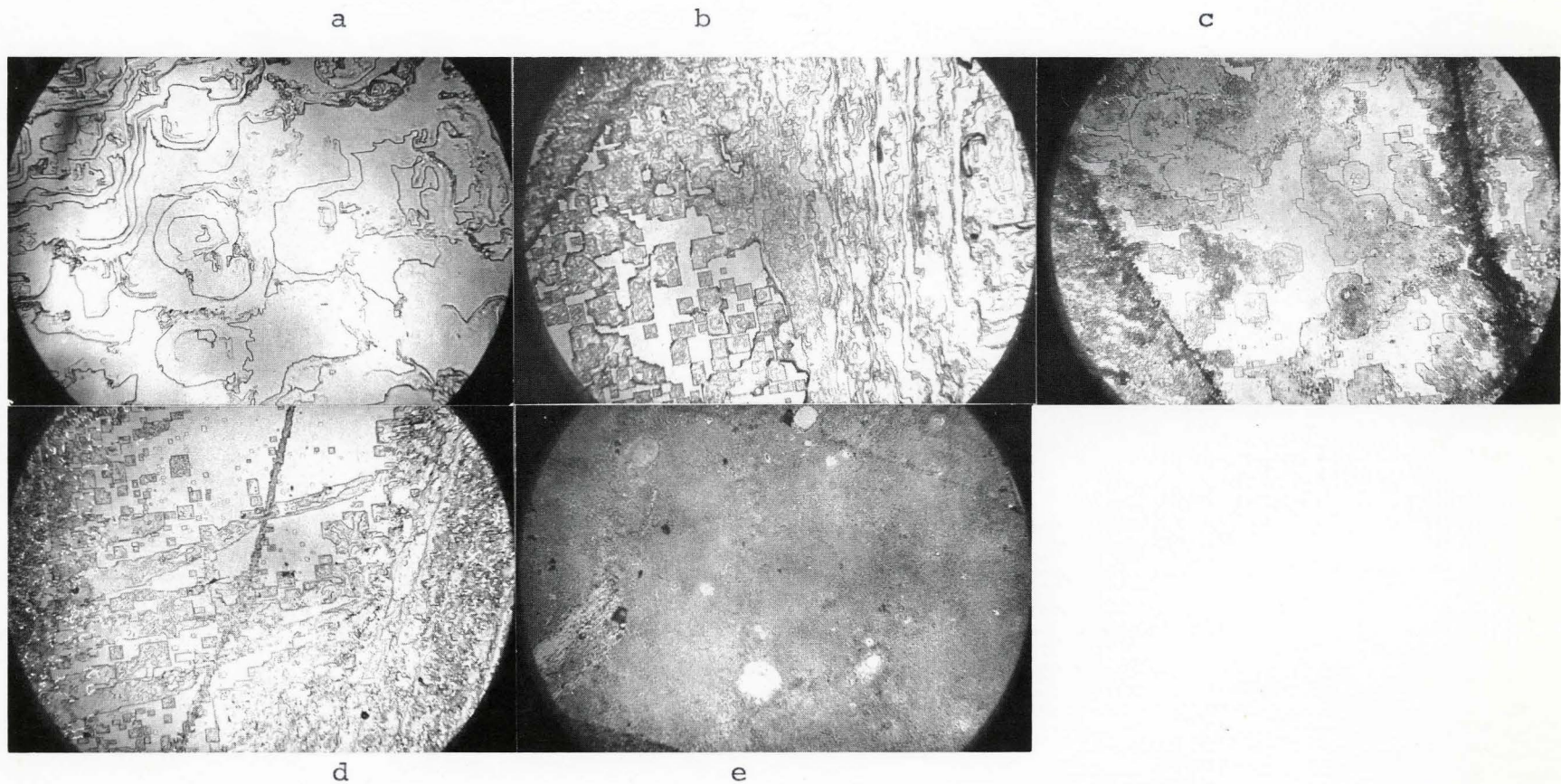


Figure 17: Optical micrographs of lithium fluoride surfaces etched 2 minutes with stirring in

a. 1 N HCl. b. 0.1 N HCl. c. 0.01 N HCl
d. 0.001 N HCl. e. 0.001 N HCl. (270 X)

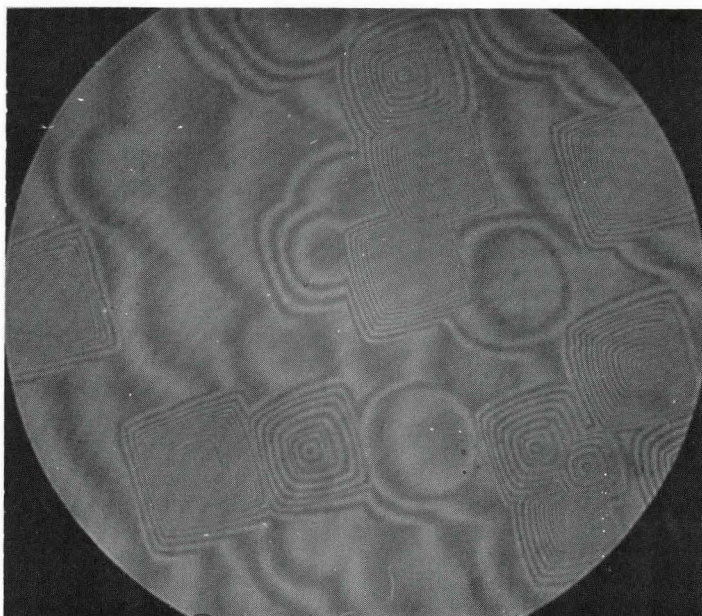


Figure 18

Interference micrograph of a lithium fluoride surface etched 2 minutes on a silica gel equilibrated with 10^4 ppm Fe^{+3} etchant (350 X)

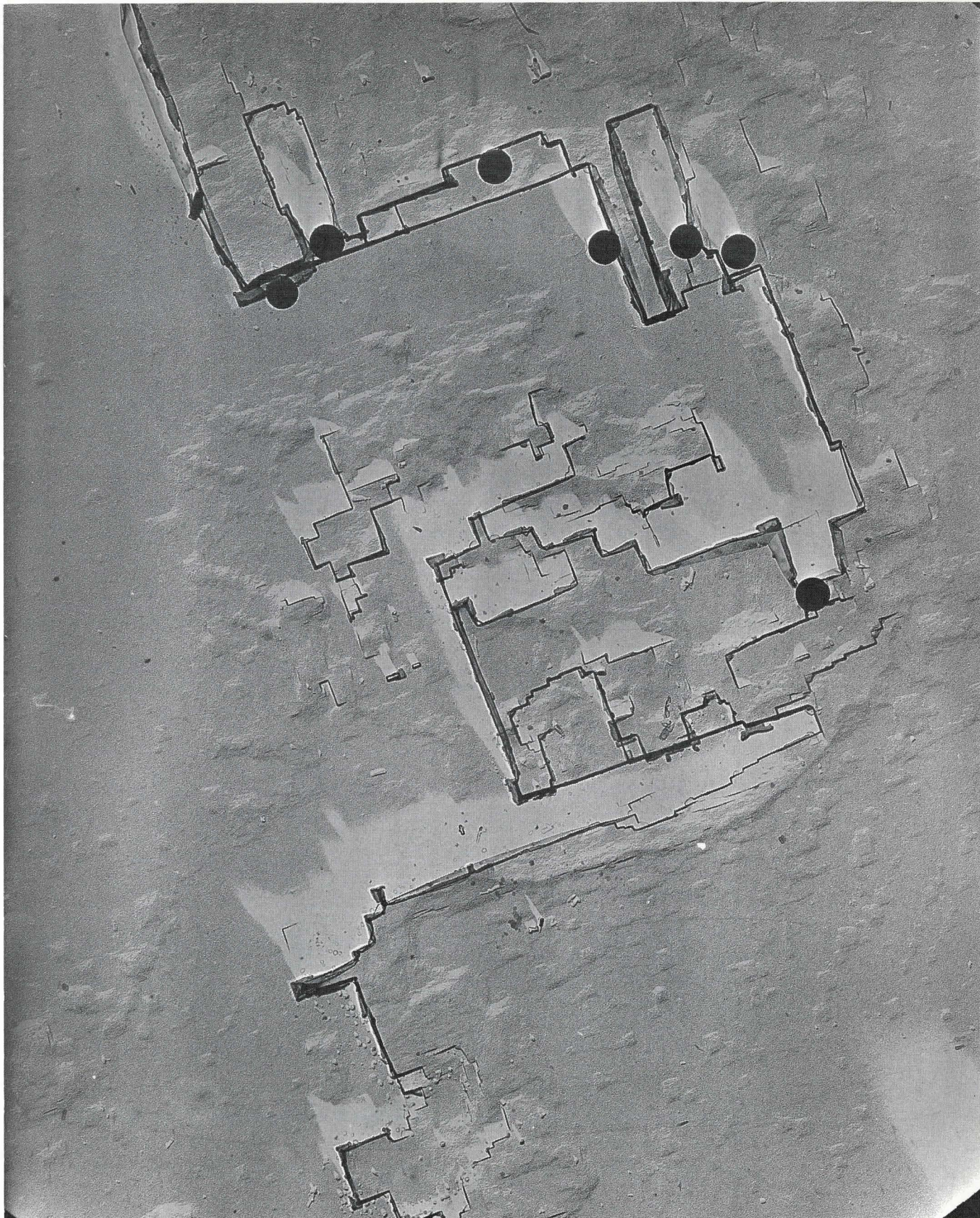


Figure 19

Palladium gold shadowed graphite replica of a lithium fluoride surface etched 2 minutes with stirring in 0 ppm Fe^{+3} etchant. (17,500 X)

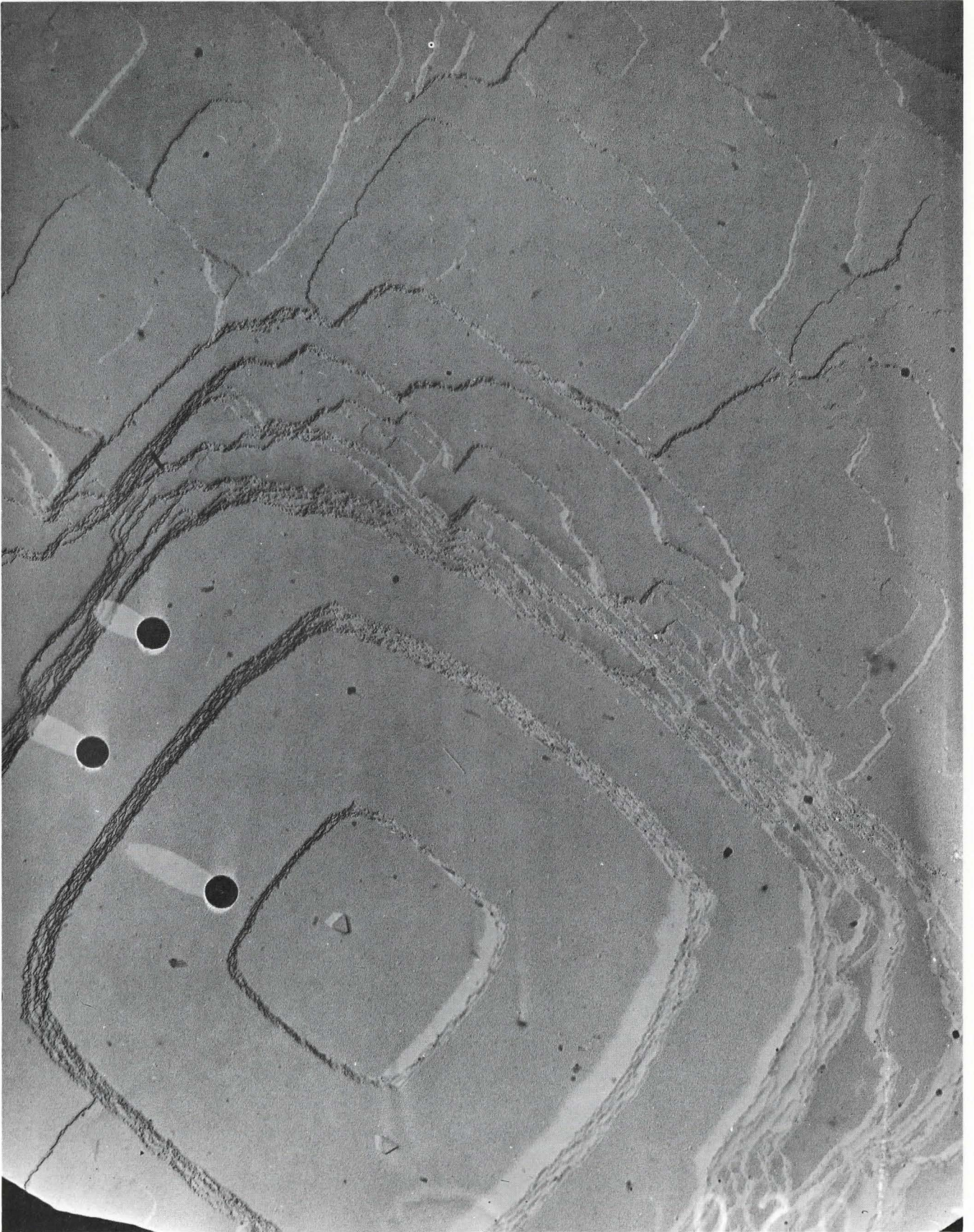


Figure 20
2 minute, 2 ppm Fe^{+3} stirred etch. (17,000 X)

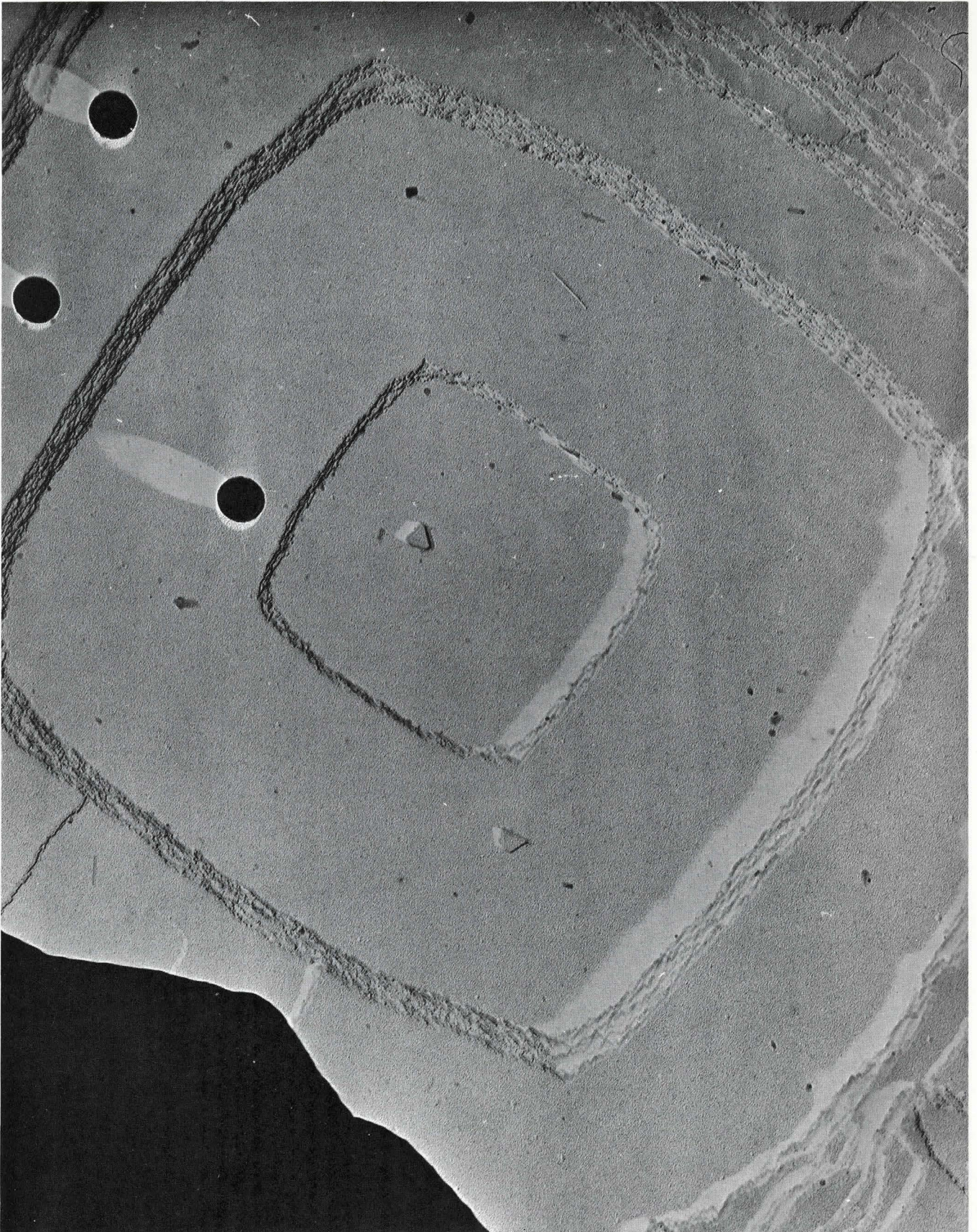


Figure 21

2 minute, 2 ppm Fe³⁺ stirred etch. (27,000 X)



Figure 22

2 minute, 5 ppm Fe^{+3} stirred etch. (17,000 X)

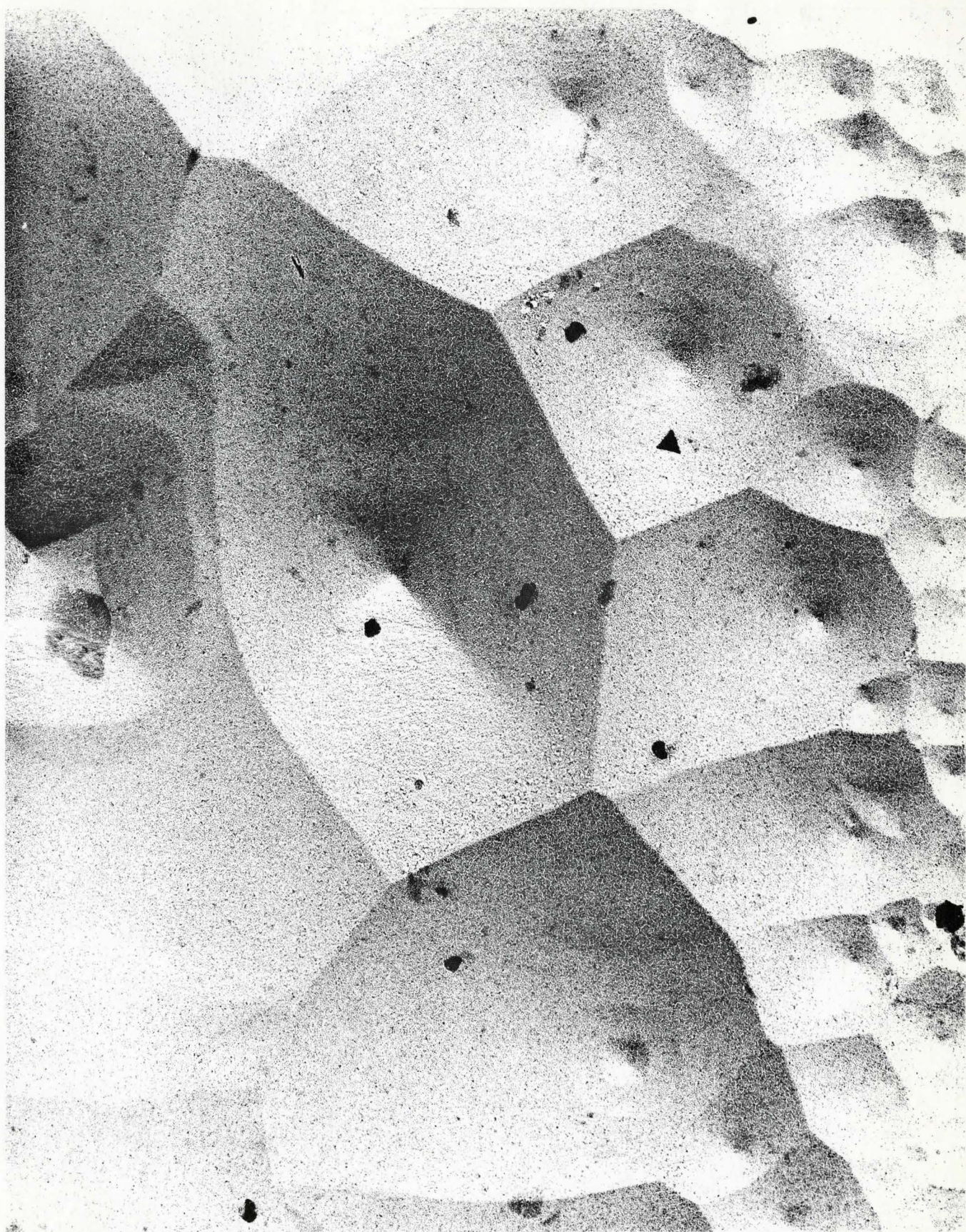


Figure 23: 30 second, 150 ppm Fe³⁺ stirred etch. (20,000 X)

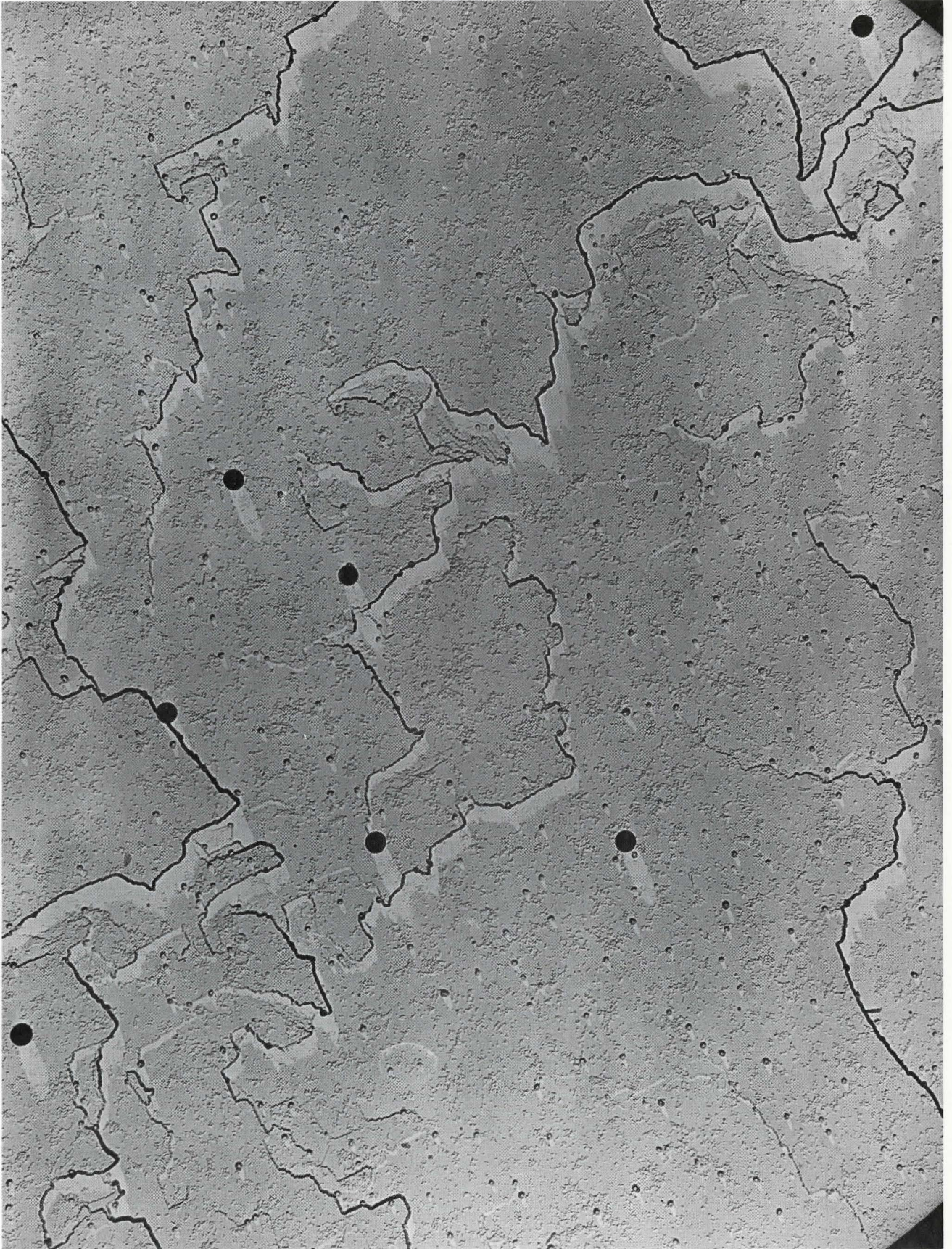


Figure 24: 5 minute, 0 ppm Fe³⁺ gel etch. (9500 X)

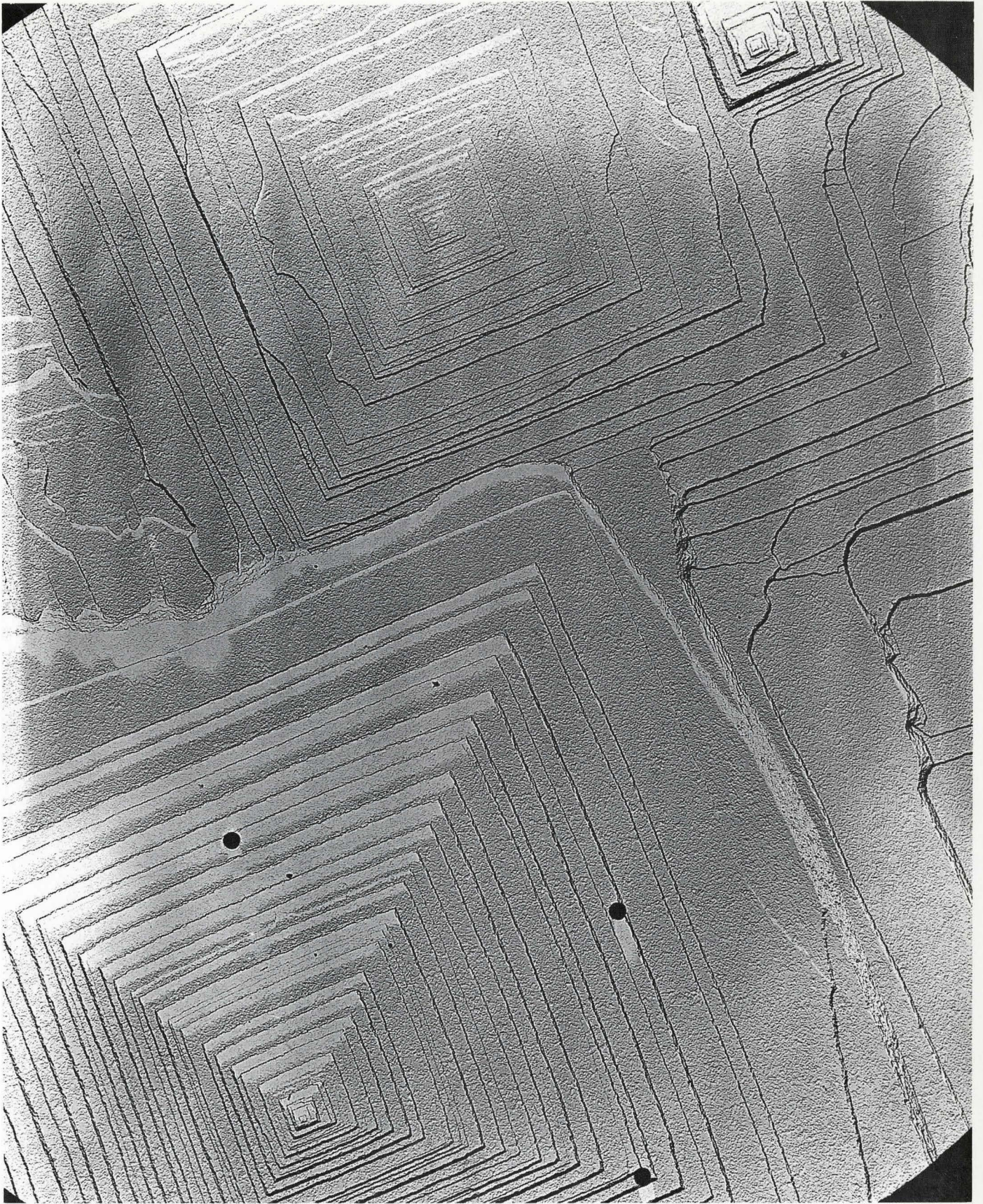


Figure 25: 2 minute, 10 ppm Fe^{+3} gel etch. (8000 X)



Figure 26: 2 minute, 10 ppm Fe^{+3} gel etch. (11,000 X)

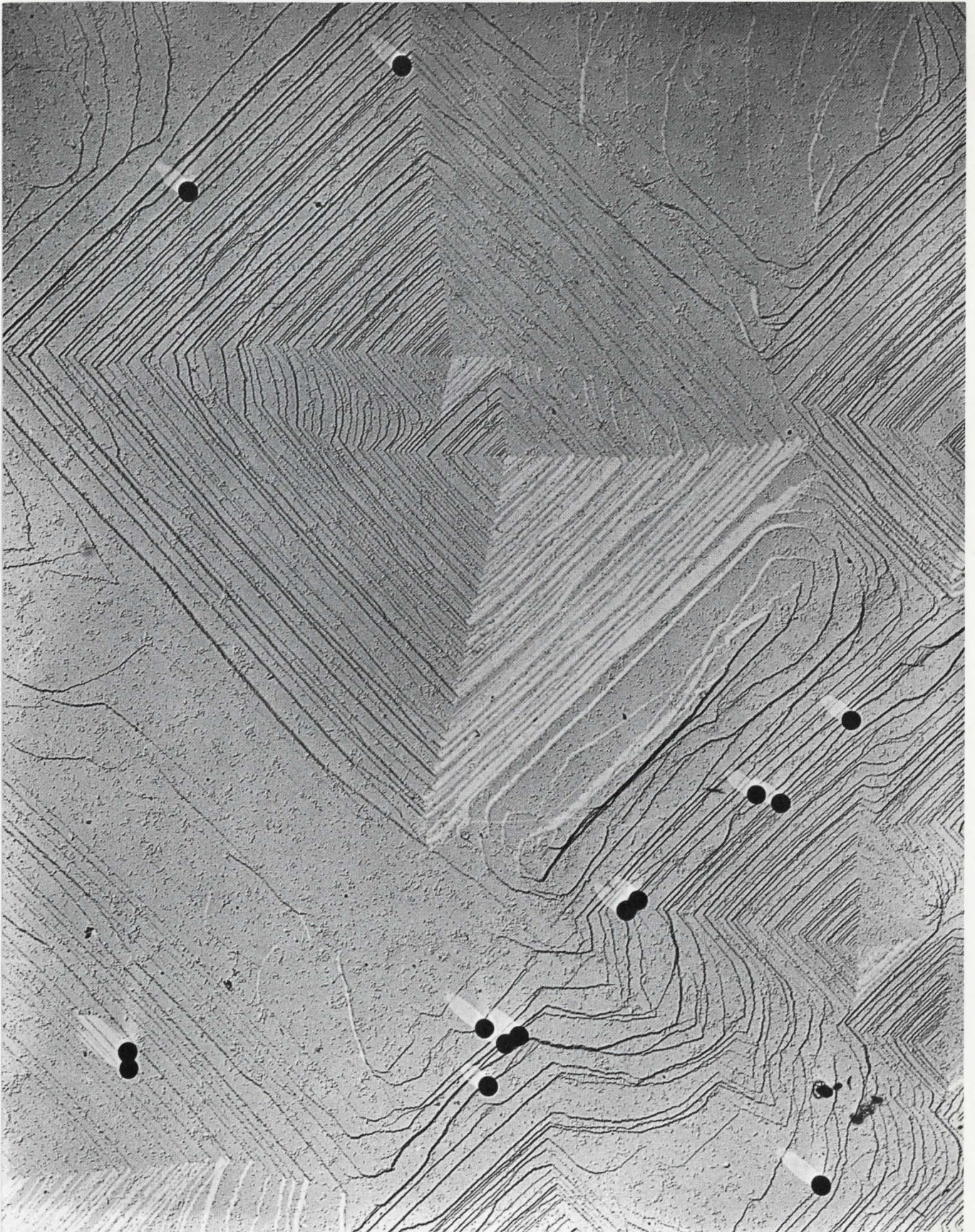


Figure 27: 2 minute, 100 ppm Fe^{+3} gel etch. (9500 X)

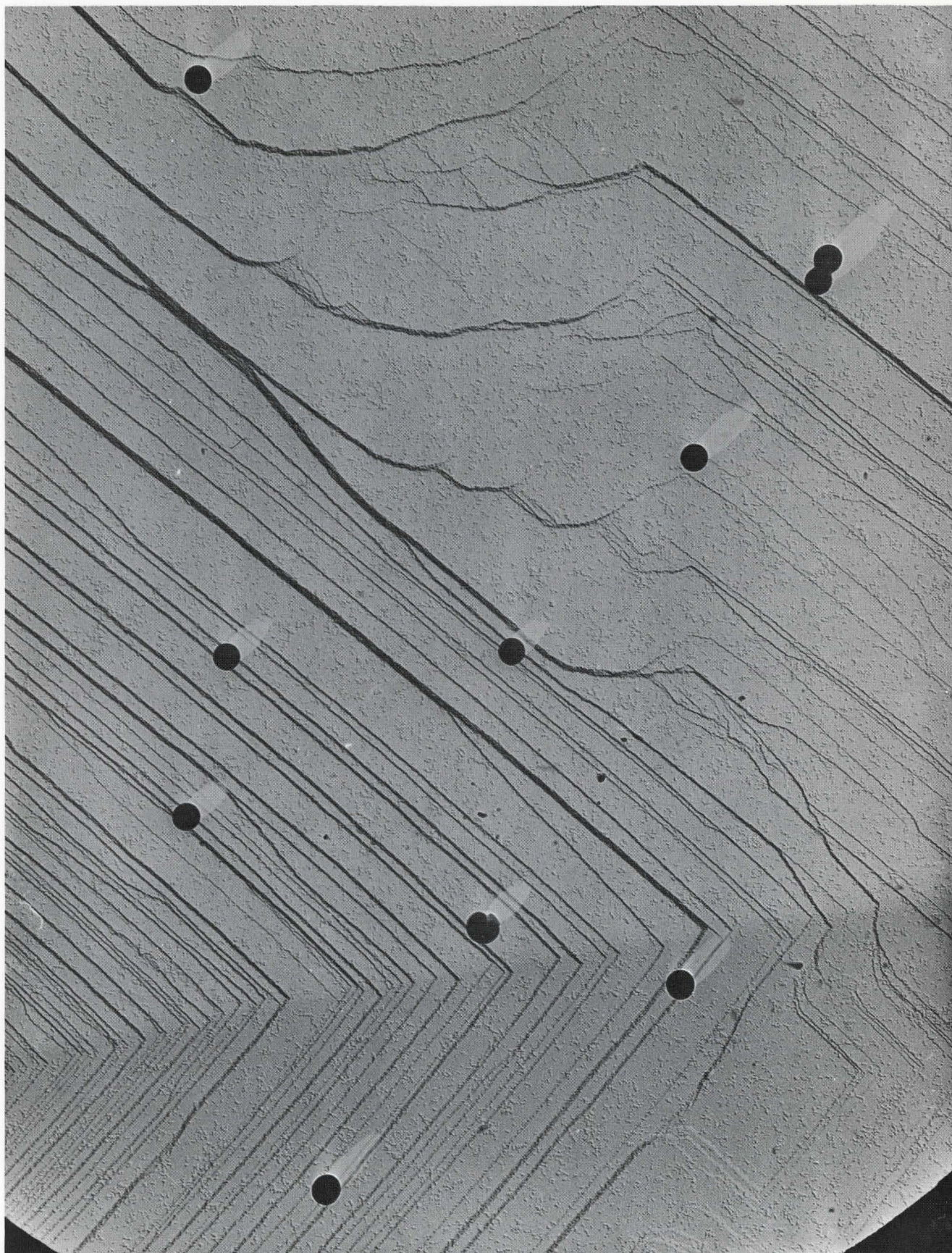


Figure 28: 2 minute, 100 ppm Fe^{+3} gel etch. (13,000 X)

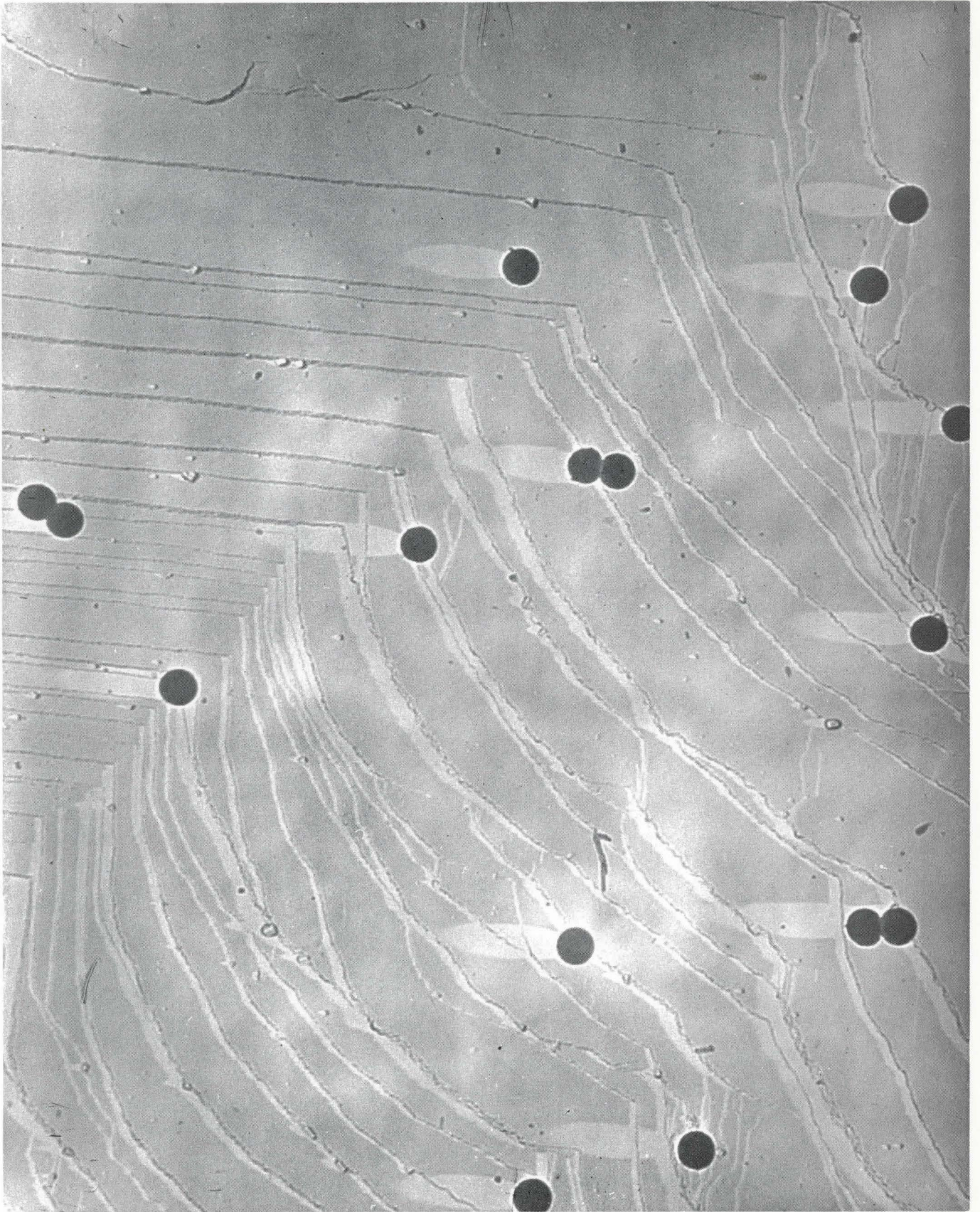


Figure 29: 2 minute, 100 ppm Fe⁺³ gel etch. (19,000 X)

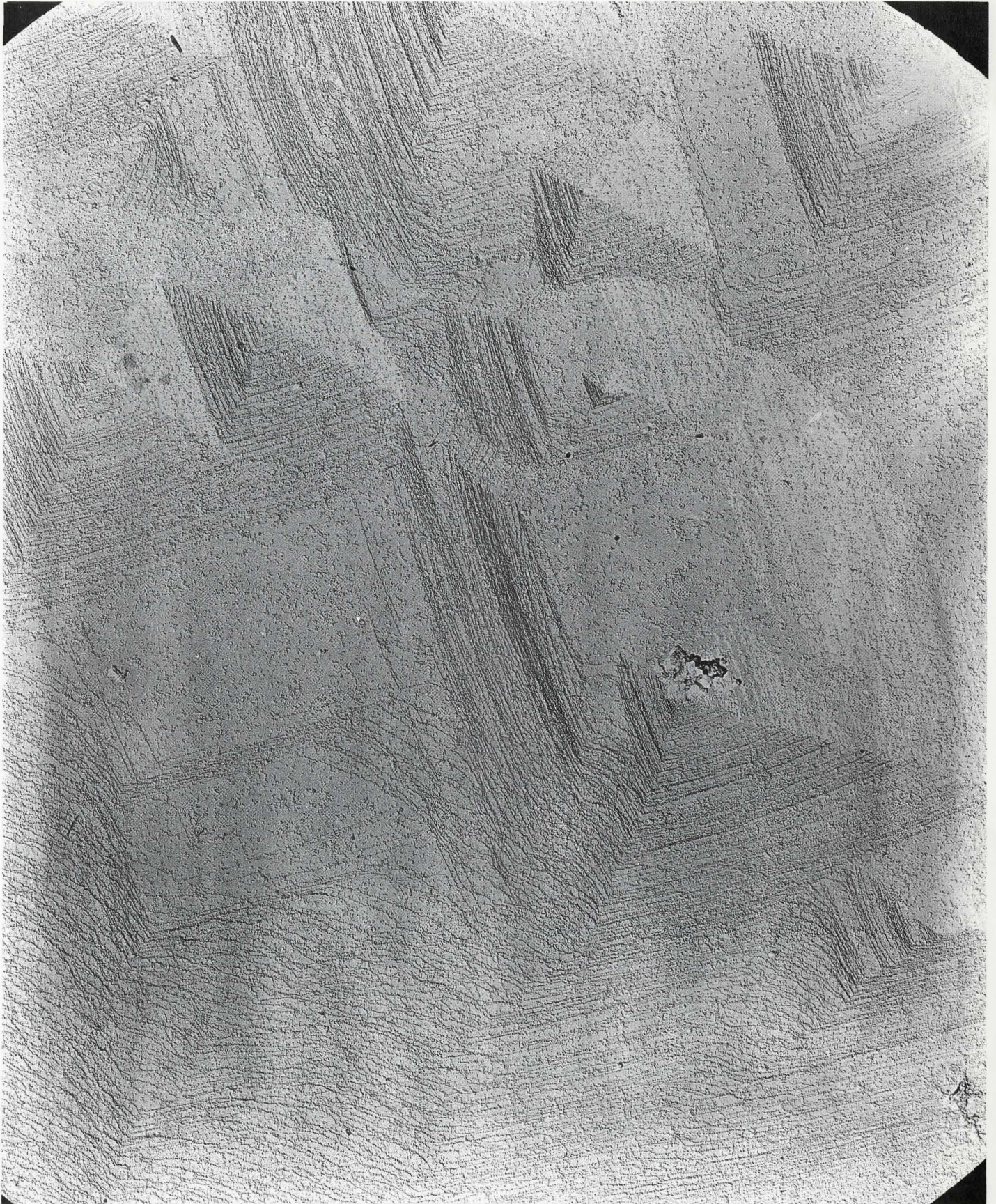


Figure 30: 5 minute, 1000 ppm gel etch (4000 x)

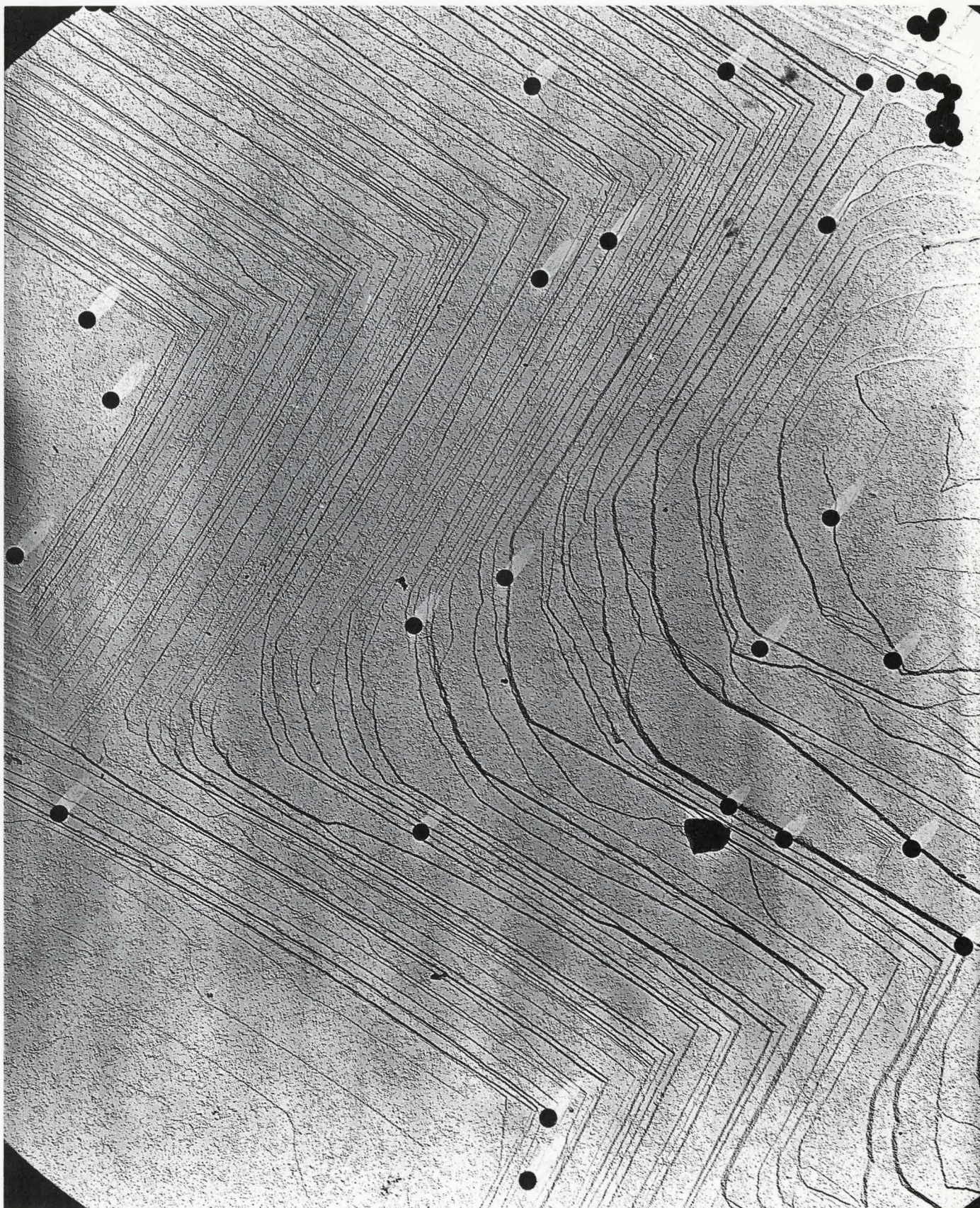


Figure 31: 5 minute, 1000 ppm Fe^{+3} gel etch. (8000 X)

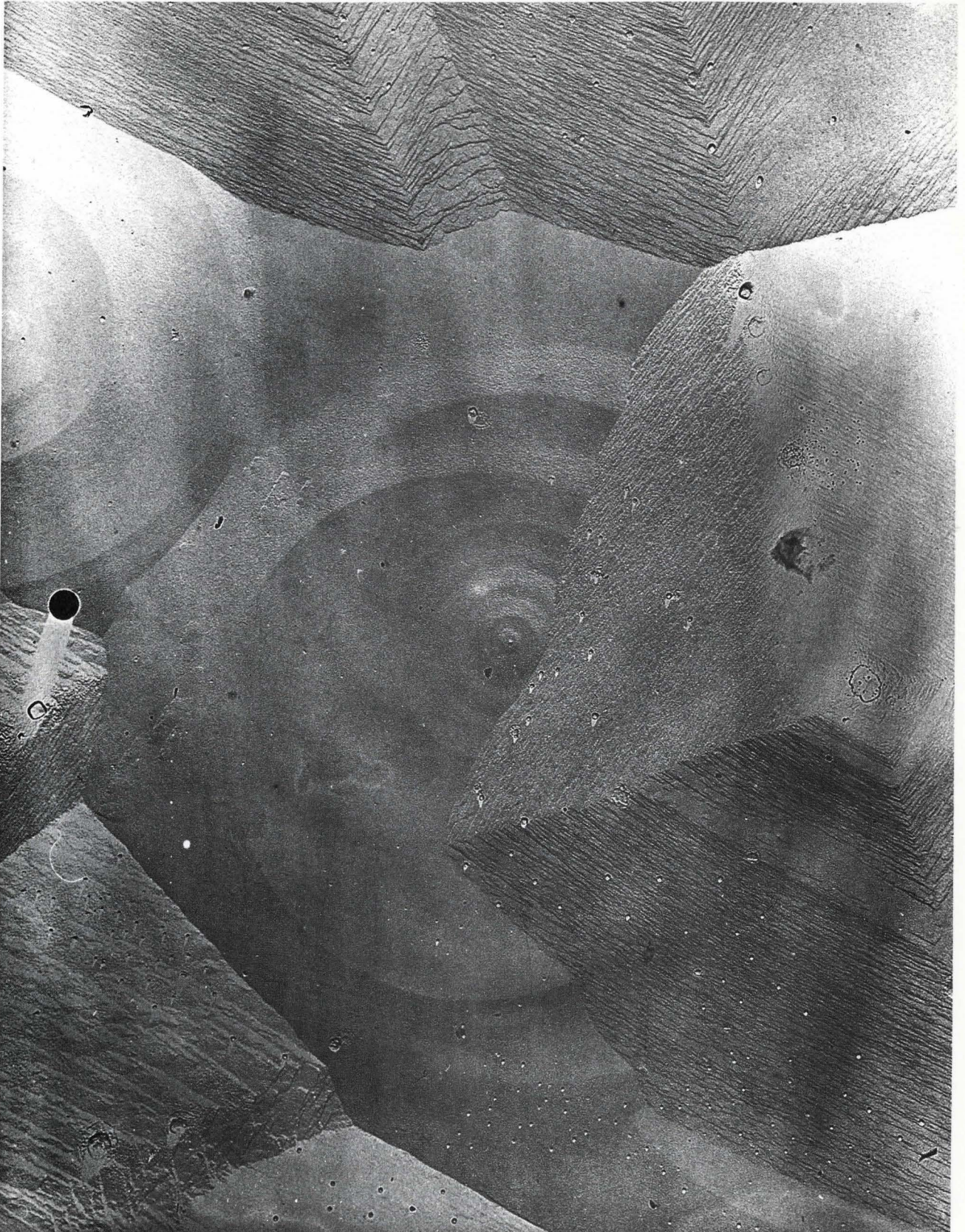


Figure 32: 2 minute, 10^4 ppm Fe^{+3} gel etch. (14,500 X)

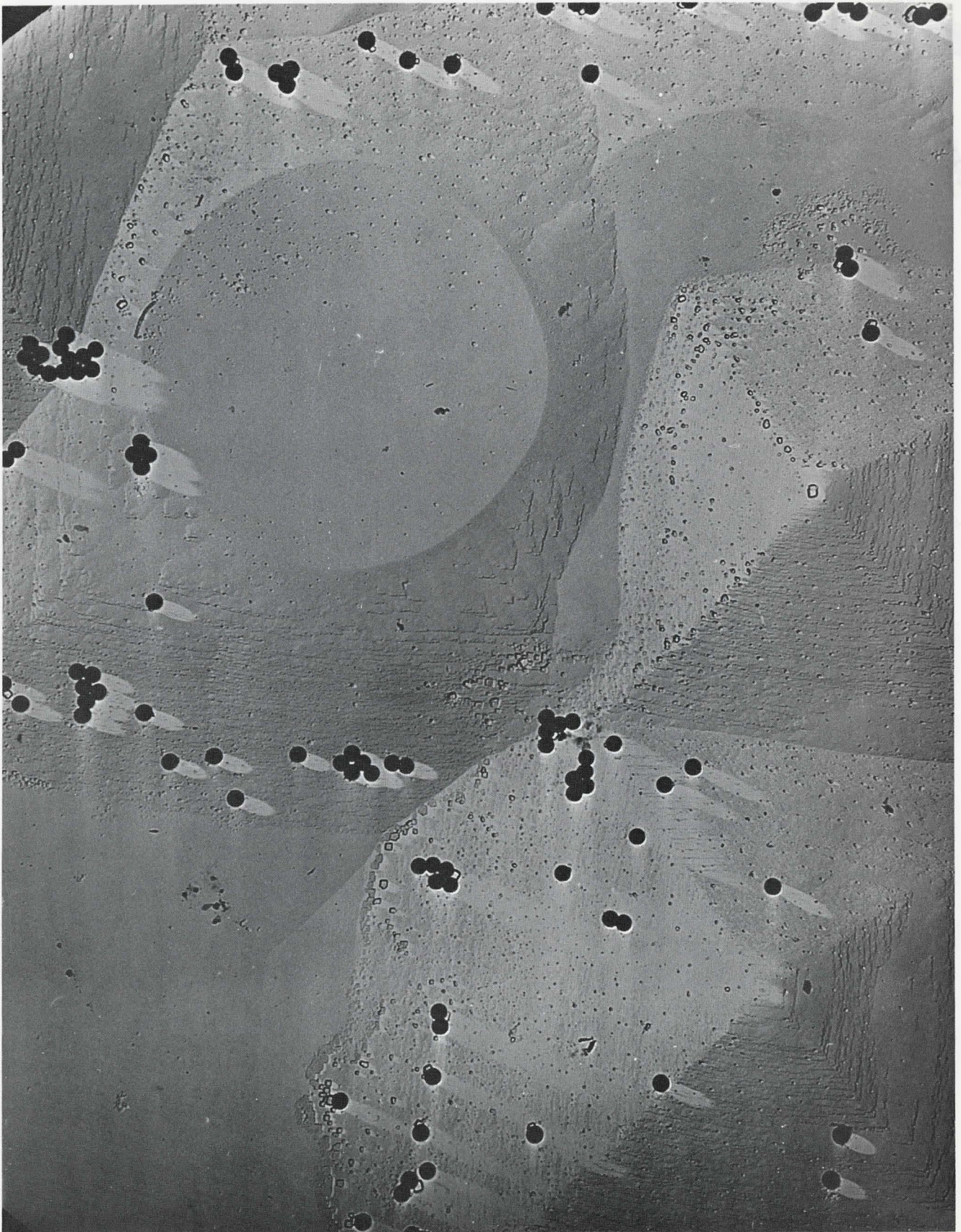


Figure 33: 2 minute, 10^4 ppm gel etch. (9000 X)